ION PAIR STRUCTURE AND BETA-CARBON STEREOCHEMISTRY IN THE ANIONIC OLIGOMERIZATION OF VINYL PYRIDINES

By

WAYLON L. JENKINS

A DISSERTATION PRESENTED TO THE GRADUATE COUNCIL
OF THE UNIVERSITY OF FLORIDA
IN PARTIAL FULFILLMENT OF THE REQUIREMENTS FOR THE
DEGREE OF DOCTOR OF PHILOSOPHY

UNIVERSITY OF FLORIDA

1978

To my wife,

Carol

ACKNOWLEDGEMENTS

The author wishes to express his thanks to all of the members of his Supervisory Committee, Dr. George Butler, Dr. John Zoltewicz, Dr. Wallace Brey, and Dr. Ronald Gordon for their assistance and support in the completion of this project. Special thanks are due to Dr. Thieo Hogen Esch for his direction and encouragement. Thanks are also due to Dr. Chao Fong Tien for many helpful discussions.

Thanks to all of the inhabitants of the fourth floor of SSRB for creating such a congenial working environment and for the studies in international relations. The world would be so much better if nations were as cooperative as their people.

Finally, thanks to the author's wife, Carol, for her love and support; she is his greatest discovery.

TABLE OF CONTENTS

LIST OF TABLES

LIST OF FIGURES

Abstract of Dissertation Presented to the Graduate Council of the University of Florida in Partial Fulfillment of the Requirements for the Degree of Doctor of Philosophy

ION PAIR STRUCTURE AND BETA-CARBON STEREOCHEMISTRY IN THE ANIONIC OLIGOMERIZATION OF VINYL PYRIDINES

By

Waylon L. Jenkins

June, 1978

Chairman: Thieo E. Hogen Esch
Major Department: Chemistry

The ion pair structures of alkali metal salts of 2-ethylpyridine were investigated using ultraviolet spectroscopy, conductimetry, ^{1}H NMR, ^{13}C NMR, and semiempirical molecular orbital calculations. The position of the cation, hybridization of the anion, charge distribution, and anion geometry were investigated.

NMR spectroscopy revealed that the interconversion between the E and Z isomers of the 2-ethylpyridyl anion is slow on the NMR time scale at temperatures below 100°C. The equilibrium between the two isomers was found to be cation and solvent dependent. The E isomer is favored by smaller cations and poorer cation solvating media. The

equilibrium showed essentially no dependence on temperature, indicating that ΔH is negligible, and that the equilibrium is primarily controlled by entropy.

The charge distribution as obtained from MO calculations and correlations with ^{13}C NMR spectra show the anion to be essentially ambident, with charge concentrated at Cα and N. The large charge density on N is consistent with sp^2 hybridization at Cα as indicated by ^{13}C NMR and MO calculations. The preferred cation position appears to be between Cα and N, above the plane of the carbanion.

Beta-deuterated 2-vinyl- and 4-vinylpyridine monomers were synthesized to study the beta-carbon stereochemistry in the anionic oligomerization of vinyl pyridines. The findings for the stereochemistry of addition of 2-vinylpyridine to Li and K salts of 2-ethylpyridine correlate very well with the relative proportions of the anion geometries in each case. Trimeric and tetrameric products were also isolated to study the effect of penultimate and antepenultimate groups. Addition of beta-deuterated 4-vinylpyridine to the Li salt of 2-ethylpyridine showed no selectivity at the beta-carbon. A model is discussed for the addition of 2-vinylpyridine to 2-alkylpyridyl salts which incorporates the ion pair structure of the 2-alkylpyridyl salt and coordination of approaching monomer with the cation.

Chairman

CHAPTER I

INTRODUCTION

Anionic polymerization of vinyl monomers is much more involved than Equation 1 would indicate. For a given monomer,

Equation 1

effects of counterion, solvent, and temperature can result in drastic changes in the polymerization process by altering the nature of the propagating species (1,2). The propagation may occur through free ions, a variety of ion pairs, or higher aggregates. Kinetic investigations of the anionic polymerization of styrene, dienes, vinyl pyridines, and some acrylates and methacrylates have yielded information about the relative reactivities of various propagating species (3,4). The propagation rate constants of free ions of living polystyrene at 25°C do not vary by more than a factor of 2 from the value of 6×10^4 M^{-1}, whatever the aprotic solvent, although the rate constants of the ion pairs vary by more than three orders of magnitude as solvent and counterion are changed (1, 2). Further investigations indicated that this variation was due primarily to the participation of two species: loose or solvent separated ion pairs which have propagation rate constants only slightly smaller than the free ions, and

tight or contact ion pairs which are much less reactive (5-7). Thus, the wide variations in reactivities represent primarily changes in the proportions of solvent separated ion pairs. In dioxane, where propagation appears to be mostly through contact ion pairs, an additional cation effect is found where the reactivity varies in the order $Li^+ < Na^+ < K^+ < Rb^+ < Cs^+$ (8-10). This variation in a series in which all of the ion pairs are tight suggests participation of the cation in the process, and has been explained by a "push-pull" mechanism as illustrated (1).

Here the cation aids in polarization of the incoming monomer. This mechanism is affected by the relationship between the cation-anion and cation-solvent interactions. In a poor solvent, small cations may form very tight ion pairs which require considerable stretching of the anion-cation distance in the transition state. The energy required for stretching reduces the net effectiveness of the cation's pull. Thus, if the energy required for stretching increases faster with decrease in ionic radius than the strength of the pull, the observed trend would result. From this discussion it is apparent that a detailed understanding of ion pair structure is required in order to understand completely the mechanism of anionic polymerization.

In addition to cation and solvent effects upon the ion pair structure, the effect of the polymer chain is of interest. For example, the dissociation constant, K_d, of polystyrene capped with a 2-vinyl pyridine unit is less than the K_d of poly-(2-vinyl)pyridine (12). This was explained on the basis of solvation by the penultimate group as illustrated.

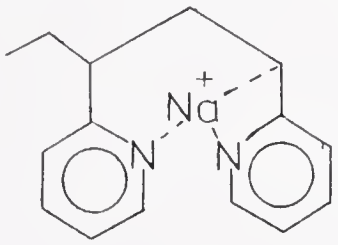

Although kinetic and conductimetric investigations have provided much insight into anionic polymerization, the stereochemistry requires a more detailed understanding of the mechanism. For monosubstituted vinyl monomers only alpha-carbon stereochemistry can be studied.

The alpha-carbon stereochemistry may be discussed in terms of the tacticity of the polymer chain. The configuration at the chain end is determined as the bond is formed between the chain end and the approaching monomer. Stereoregular polymerization requires a mechanism for controlling the approach of the monomer to produce the correct configuration. The mechanisms proposed usually involve either steric control or solvation by the penultimate group to produce a configuration favoring one approach over the other.

In the case of monosubstituted or 1,1-dissubstituted monomers, beta-carbon stereochemistry can be studied only by preparing specifically deuterated monomers.[13] Such a monomer has two nonequivalent sides as illustrated. If the

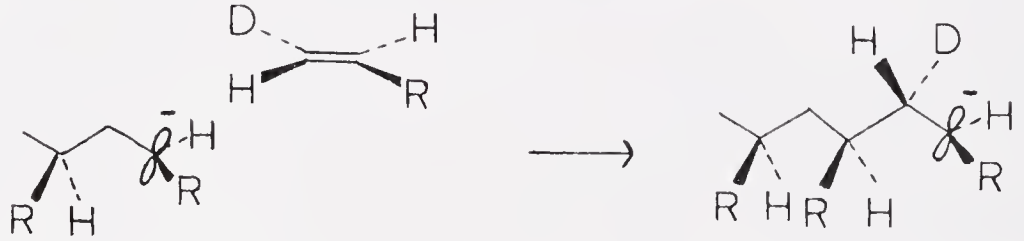

monomer approaches in a way that it presents its bottomside, as shown, to the topside of the chain, the erythro product results. The alpha-carbon stereochemistry of the chain end and the beta-carbon stereochemistry of the approaching monomer are determined simultaneously. However, for each monomer unit the alpha- and beta-carbon stereochemistry are determined at two different times and there may not be a definite relationship between the two. In principle, a given monomer may produce erythro di-isotactic polymer in which the deuterium and the substituent R are on opposite sides of the extended polymer chain, or threo di-isotactic polymer, or the polymer may be isotactic at the alpha-carbon and atactic at the beta-carbon. Of course, a syndiotactic polymer renders beta-carbon stereochemistry meaningless since the methylene protons become equivalent.

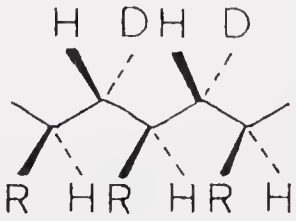

erythro di-isotactic

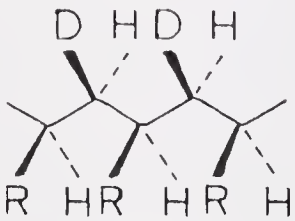

threo di-isotactic

Work by Fowells et al. has shown that a change of solvent may be sufficient to alter the beta-carbon stereochemistry while leaving alpha-carbon stereochemistry unchanged (14). At -78°C in toluene the polymerization of Z-1-deuterio-2-methyl-ethylpropenoate initiated by fluorenyllithium produces threo di-isotactic polymer. The addition of small quantities of THF (THF/RLi = 7.5) results in the formation of erythro di-isotactic polymer. The polymer produced in THF is syn-diotactic.

A simplified interpretation is illustrated in Figure 1 (13). In toluene the approach of the monomer is directed by the cation in an "isotactic-like" approach resulting in threo di-isotactic polymer. The addition of THF coordinatively saturates the cation so that the incoming monomer can no longer penetrate the solvation shell of the cation. The monomer now approaches in a more sterically favored "syn-diotactic-like" approach to produce erythro product. In order to produce isotactic polymer, rotation about the Cα-Cβ bond must occur prior to the next monomer addition. This rotation may be aided by the chelation effect to produce the proper configuration. Thus in the acrylate system, beta-carbon stereochemistry may vary while alpha-carbon stereochemistry remains constant. In fact, the Grignard-initiated polymerization of α-cis-β-d_2-acrylate leads to an isotactic polymer alternating between erythro di-isotactic and threo di-isotactic blocks along the chain, indicating that two different propagating species were interconverting during the polymerization (15).

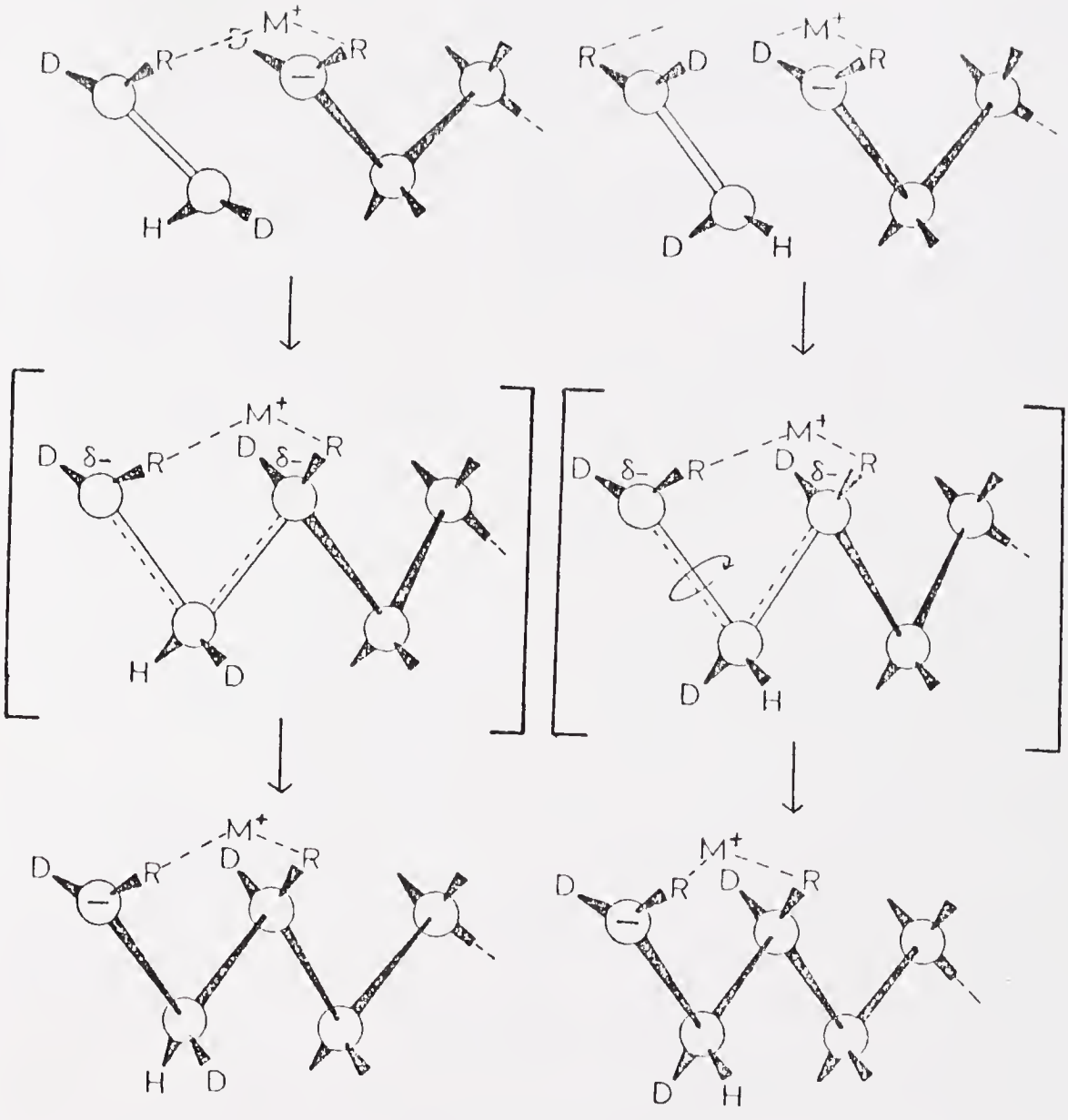

Figure 1. Monomer Approach Modes for an Isotactic Placement

A knowledge of the monomer structure of a beta-deuterated monomer and the placement in the polymer provides information about whether the formal mode of addition represents a cis or trans opening of the monomer as shown (13).

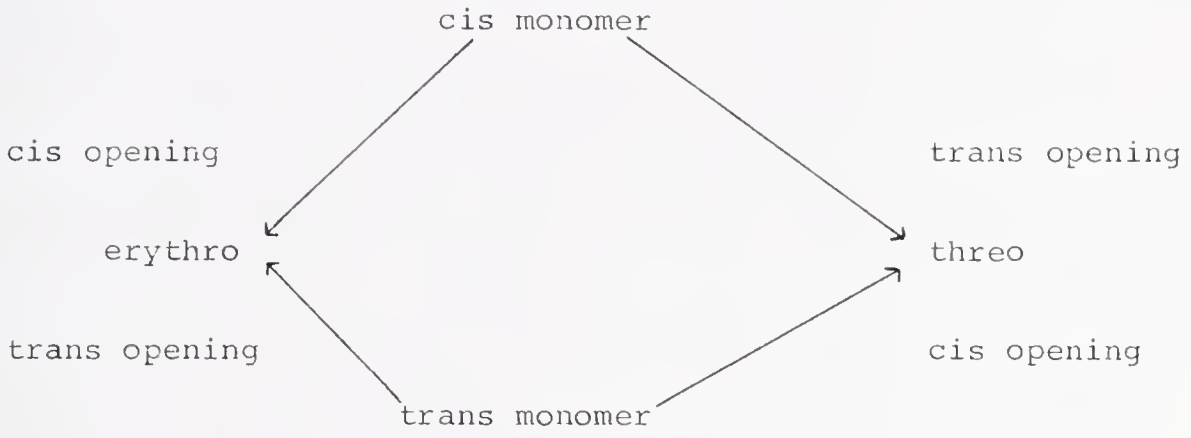

Thus, the possible relationships between alpha-carbon and beta-carbon stereochemistry raise the following questions:

1. Is the stereochemical configuration at the propagation site fixed, or is rotation around the Cα-Cβ bond free?

2. If the geometry at the chain end is maintained, does the monomer approach from one side preferentially, or is it free to attack from either side?

3. If the geometry is maintained, and monomer approaches preferentially from one side, does the presentation favor one face of the monomer over the other?

Work on the anionic oligomerization of vinyl pyridines has provided answers to some of these questions. The methylation of [1] was studied according to Equation 2 (16). The

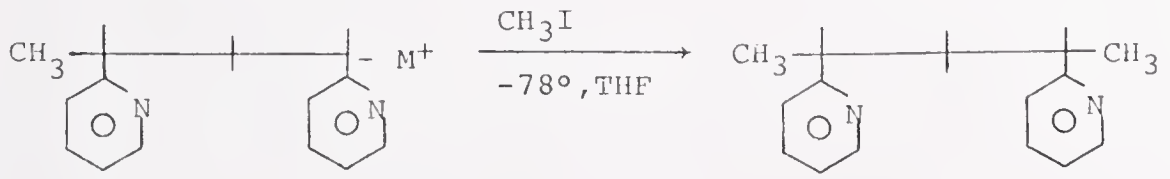

[1] Equation 2

effects of cation, solvent, and solvating agent upon the methylation stereochemistry are shown in Table 1. The stereoselectivity increases with decreasing cation radius. Also, the addition of strongly cation solvating agents such as 18-crown-6 results in loss of selectivity. Furthermore, when 4-vinylpyridine was used in place of 2-vinylpyridine, the product was a 50/50 mixture of meso and racemic compounds.

These results were explained by postulating an equilibrium between two diastereomeric contact ion pairs 2a and 2b, corresponding to 3a and 3b, in which 2a predominates.

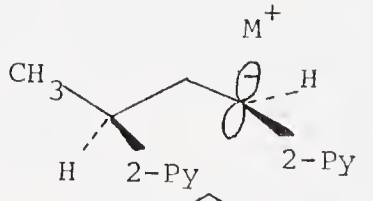

2a

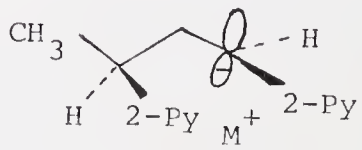

2b

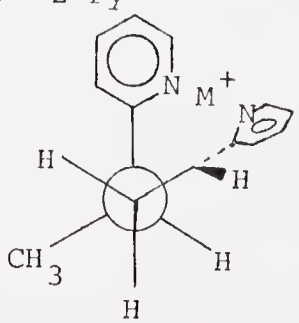

3a

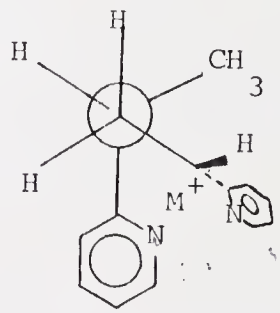

3b

Alkylation of 2a from the cation side produces the meso product. Cation side attack was assumed from earlier work on alkylation of carbanions (17a-d) and because attack from the opposite side would produce a product-separated ion pair (1, 2, 18), which should be unfavorable under the conditions of the experiment.

The work was extended to the trimer with the results shown in Table 2 (19). The trimer findings and unpublished results for the tetramer (20) indicate that the addition of

Table 1. The Methylation Stereochemistry of 1,3-Di-(2-pyridyl)butane Anion

M^+/Solvent	Temperature °C	% Meso
Li/THF	-78	>99
Li/THF	0	95
Na/THF	-78	96
K/THF	-78	65
Rb/THF	-78	57
NaCE[a]/THF	-78	58

[a]18-Crown-6 present in approximately equimolar quantity.

Table 2. The Stereochemistry of Formation of 2,4,6-Tri-(2-pyridyl)heptane

	MM	MR(RM)	RR
Li, THF	>95	<5	<5
Na, THF	>95	<5	<5
Na, THF, Na, CE, THF[a]	∿50	∿50	--
t-BuOK/DMSO[b]	∿25	∿50	∿25

[a]18-Crown-6 present during methylation.

[b]Epimerization of isotactic trimer for about 2 weeks in t-BuOK/DMSO at 25°C.

2-vinylpyridine occurs with the same stereochemistry as methylation to produce isotactic oligomers.

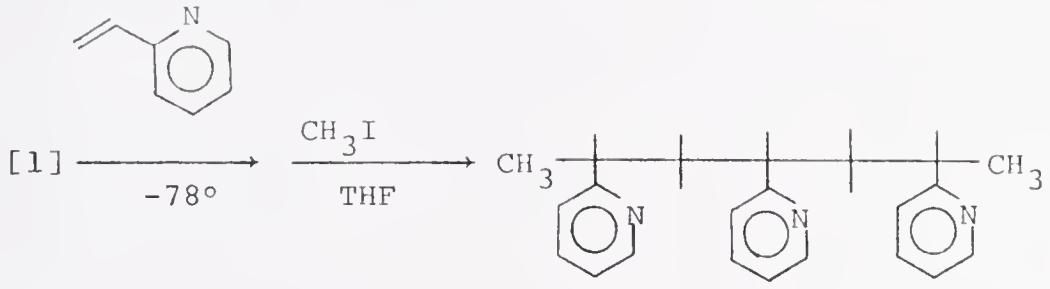

The purpose of this study is to further define the mechanism of anionic polymerization of 2-vinylpyridine using a three-pronged approach.

1. To study the ion pair structure in terms of cation position, hybridization at Cα, and charge distribution using CNDO/2 calculations.

2. To study directly the carbanionic species involved in propagation using ^{1}H and ^{13}C NMR to gain information concerning charge delocalization and the degree of double bond character in the C2-Cα bond.

3. To study the question of mode of presentation of monomer using deuterated monomers and to relate, if possible, the mode of presentation to ion pair structure.

CHAPTER II

ION PAIR STRUCTURE

Results

In discussing ion pair structure several parameters need to be determined, such as carbanion hybridization, charge distribution within the anion, anion geometry, cation position, and tightness of the ion pair. These questions have been investigated for the alkali salts of 2-ethylpyridine using ^{1}H and ^{13}C NMR, CNDO/2 calculations, UV spectroscopy and conductimetry.

UV and Conductance

The Na salts of 2-ethylpyridine (2EP) and 1,3-di-(2-pyridyl)butane (DPB) were investigated using UV and conductimetric techniques. The UV spectra of both salts matched those of living poly-(2-vinylpyridine) reported by Tardi and Sigwalt (21) and by Fisher and Szwarc (11). The maxima at 132 nm were assumed to have the same molar absorptivity as living poly-(2-vinylpyridine) (ε = 10,400). A second, much smaller maximum was observed at longer wavelengths ($\lambda_{max} \simeq 475$), similar to that attributed to impurities (21, 22). Conductance data were taken over the concentration range from 10^{-3} M to 10^{-7} M. Kraus-Brey plots of $1/\lambda$ vs. ($C\lambda$) were made and the dissociation constants obtained were 1.9×10^{-10} for Na2EP and 6.7×10^{-10} for NaDPB. The K_d for NaDPB is questionable, however, since the conductance of the solution

increased with time, indicating the presence of a side reaction not observed in the case of Na2EP. Since the two carbanions should be very nearly the same in terms of reactivity, it seems likely that this phenomenon was caused by an intramolecular reaction (21,22). The plots showed significant deviations from linearity at higher concentrations as shown in Figure 2, suggesting the formation of triple ions. For triple ions in low polarity media, the conductance equation may be written as

$$C\Lambda^2 = \Lambda_0{}^2K_1 + (2\Lambda_0\lambda_0 - \Lambda_0{}^2)K_1C/K_2$$

where Λ is the observed equivalent conductance, Λ_0 is the sum of the equivalent limiting conductances of the cation and anion and λ_0 is the equivalent limiting conductance for the triple ion (23). K_1 and K_2 are the dissociation constants of the ion pair and the triple ion, respectively. From this equation K_1 may be obtained from a plot of $(C\Lambda^2)$ vs. C which has an intercept equal to $\Lambda_0{}^2K_1$. Such plots in these systems show good linearity as shown in Figure 3, and yield values of dissociation constants for Na salts of 2EP and DPB of 1.8×10^{-10} and 6.3×10^{-10}, respectively, in good agreement with the values obtained from the Kraus-Brey plot (see Table 3). From the slope of the triple ion plot, it is possible to estimate a value for K_2. The value obtained for K_2 of 6.1×10^{-4} indicates that triple ion formation is not extensive.

In very dilute systems the absorbance of Na2EP decreased rapidly with time. Pseudo first order rate constants were calculated for the decomposition in THF and in the presence

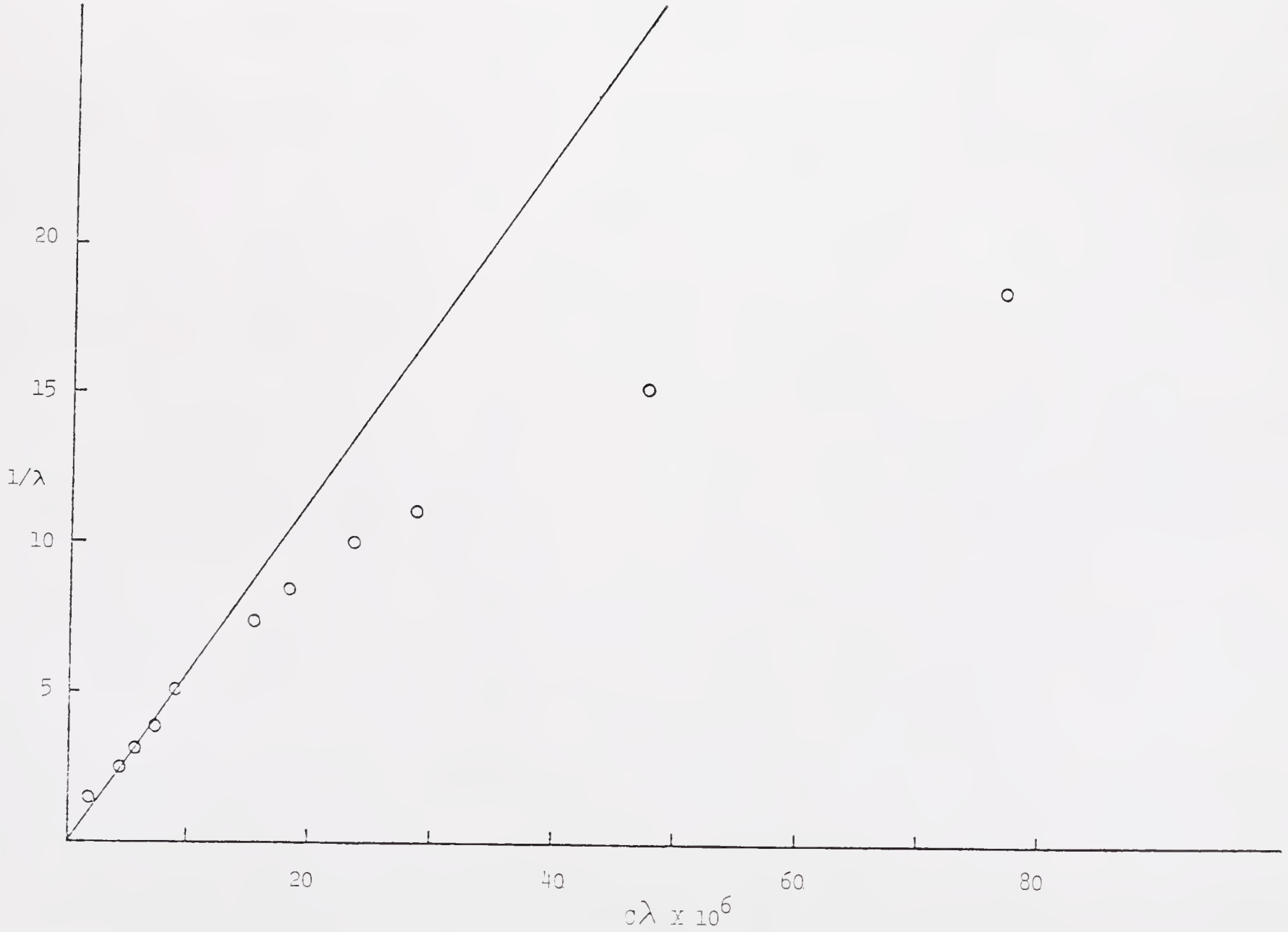

Figure 2. Kraus Brey Plot of Na2EP in THF

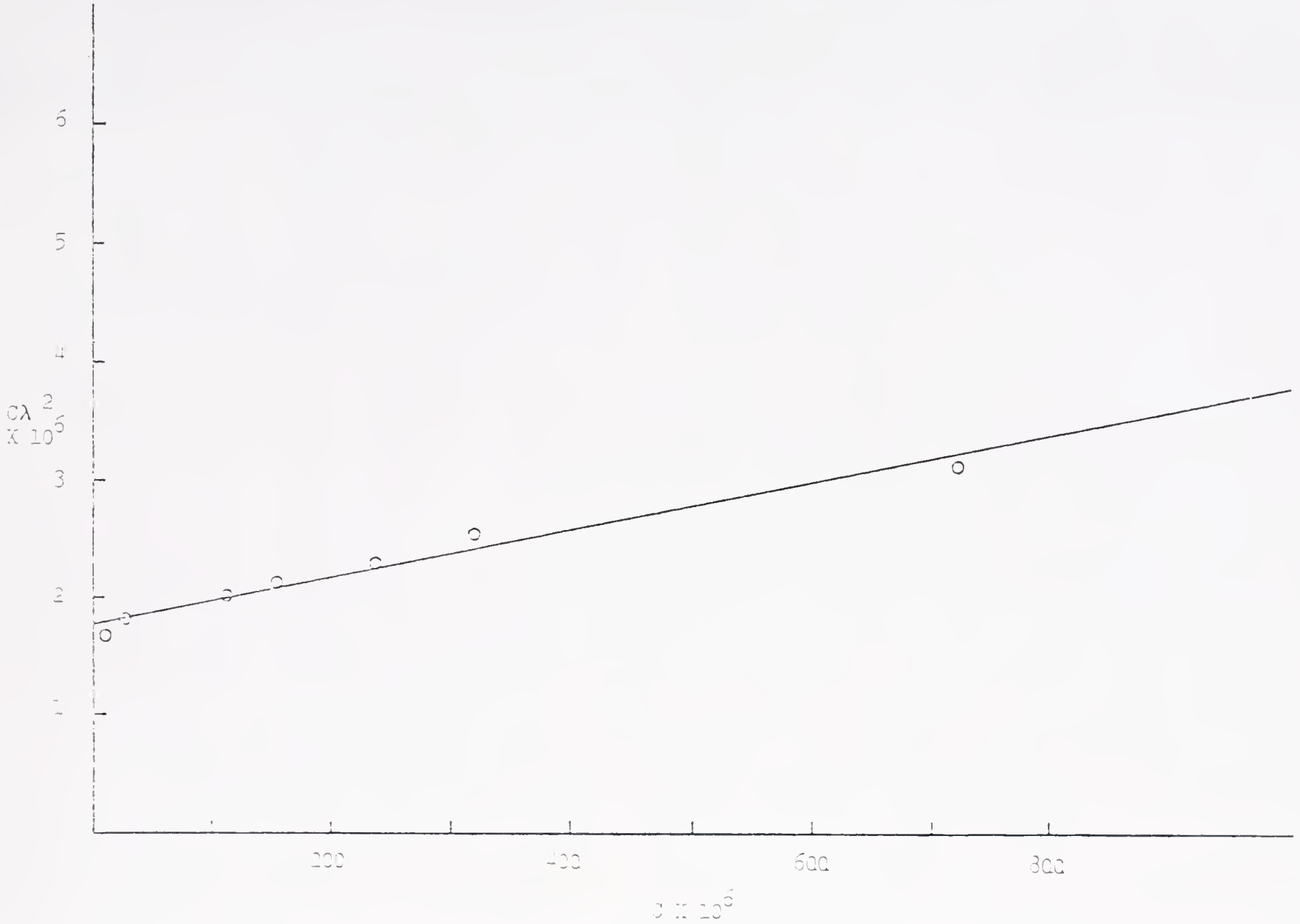

Figure 3. Triple Ion Plot of Na2EP in THF

Table 3. Dissociation Constants, K_d, of 2-Pyridyl Carbanions

Salt	Solvent	K_d
Na2EP	THF	1.4×10^{-10}
	THF/dibenzo-18-crown-6	1.5×10^{-9}
	THF/[2.2.2] cryptand	5.5×10^{-7}

of dibenzo-18-crown-6 and [2.2.2] cryptand and are shown in Table 4.

To investigate the effect of cation solvating agents, dibenzo-18-crown-6 and [2.2.2] cryptand were added to Na2EP. Following the addition of dibenzo-18-crown-6, the dissociation constant, K_d, increased approximately 10-fold as shown in Table 3. Addition of cryptand was much more dramatic, increasing the K_d by a factor of 4000. In both cases, the addition of solvating agent increased the rate of decomposition as shown in Table 4. The addition of crown resulted in no observable change in the UV spectrum. However, the addition of cryptand resulted in a shift in λ_{max} from 321 nm to 328 nm (Figure 4). Addition of excess carbanion produced a spectrum in which maxima at both 315 nm and 327 nm were observed for the uncomplexed and complexed salt, respectively.

^{1}H NMR Results

Information about anion geometry and charge distribution can be obtained by using ^{1}H and ^{13}C NMR. The spectra of the Li and K salts are shown in Figures 5 and 6. The ^{1}H NMR spectrum of the Li salt clearly shows the ring protons spread over a wide range in the order H6, H4, H3, H5 with H5 the farthest upfield. Inspection of the K spectrum reveals a second set of absorptions, with the difference being most obvious at H4. This observation is consistent with the presence of two ion pairs with differing anion geometries as indicated in Equation 3. The structures were assigned

Table 4. Pseudo First Order Rate Constants for the Decomposition of Na2EP at 25°C

	Conc. Range (M)	K_d (sec^{-1})
Na2EP	$2\text{-}3 \times 10^{-6}$	2.4×10^{-5}
Na2EP + 18-Cr-6	$1\text{-}2 \times 10^{-3}$	6.1×10^{-5}
Na2EP + [2.2.1]	$1\text{-}3 \times 10^{-3}$	5.0×10^{-4}
Na1,3DPB		1.0×10^{-5}

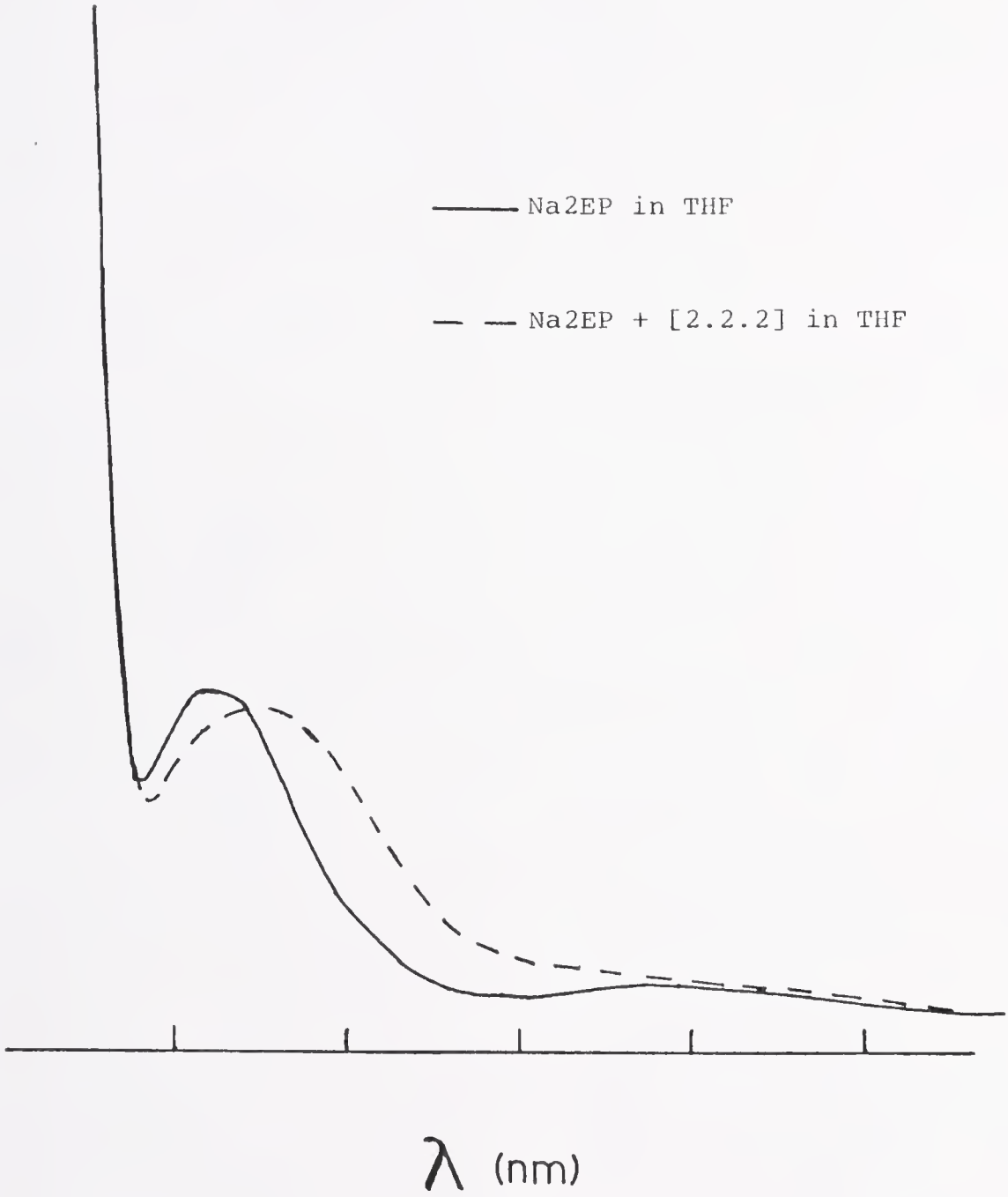

Figure 4. UV Spectra of Na2EP

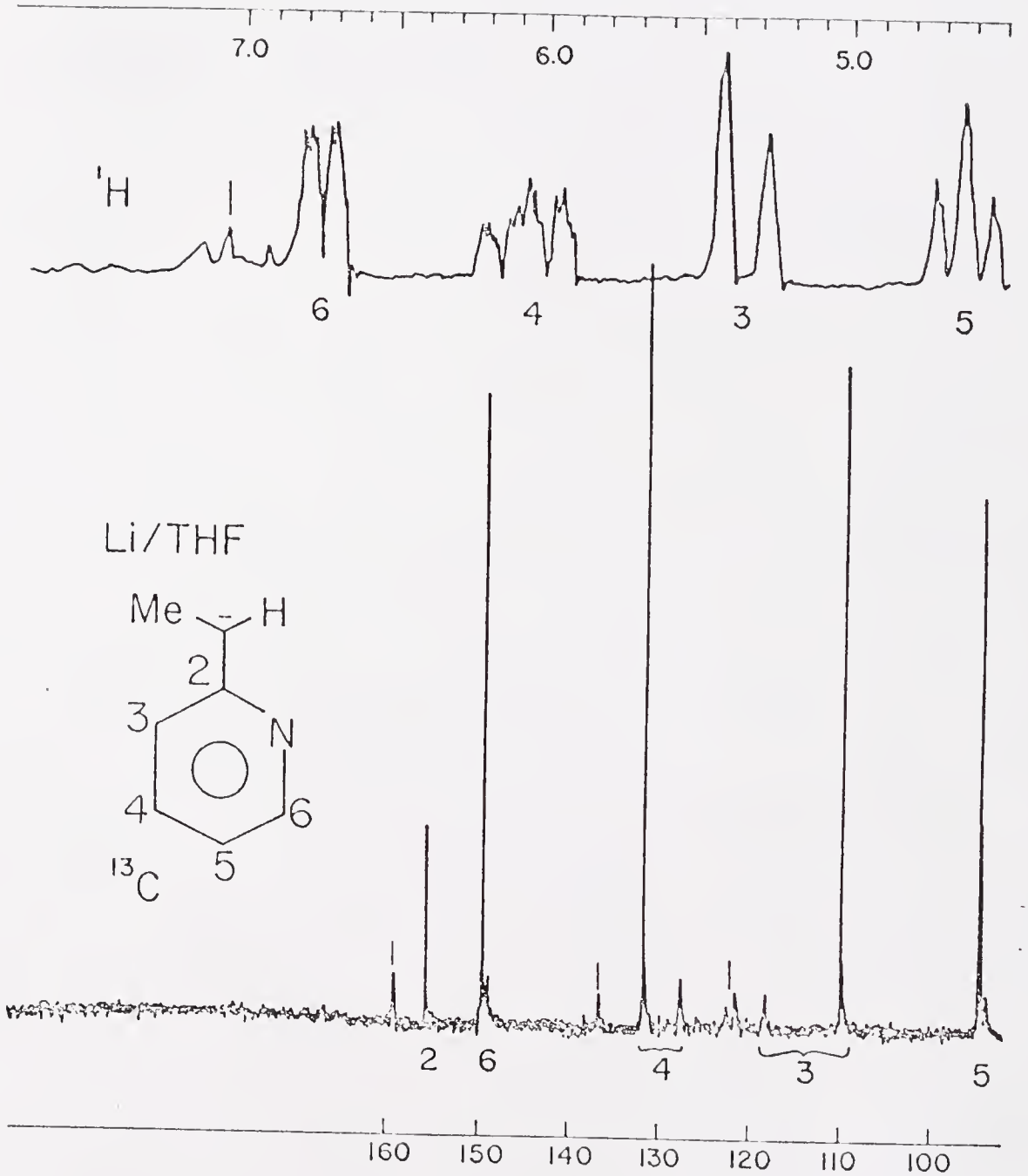

Figure 5. ^{1}H and ^{13}C NMR Spectra of Li2EP in THF

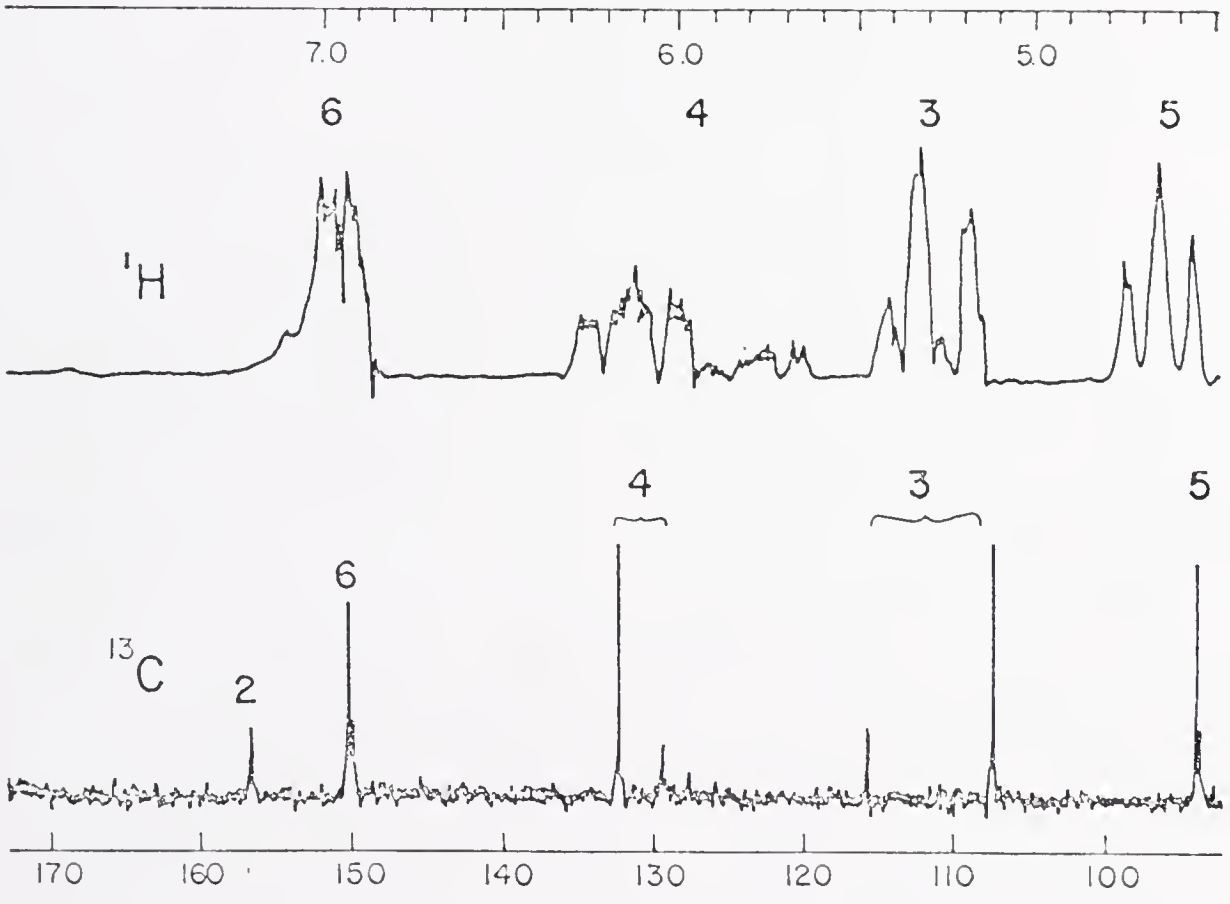

Figure 6. ^{1}H and ^{13}C NMR Spectra of K2EP in THF

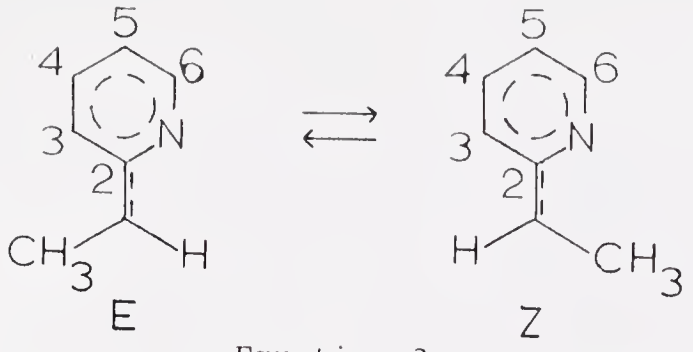

Equation 3

on the basis of long range coupling between H4 and Hα which is larger in the E isomer form as shown in Figure 7 for conditions in which the two isomers are present in approximately equal proportions. Similar long range coupling was observed by Takahashi et al. (24) in the 2-picolyl anion and was used to assign the nonequivalent alpha protons.

The most striking feature of these spectra is the presence of the E and Z ion pair isomers. Charge delocalization into the ring results in partial double bond character between C2 and Cα. This bonding is sufficient to produce two distinguishable forms in room temperature spectra. The equilibrium shows a substantial cation and solvent dependence as shown in Table 5. Larger cations and better cation solvents, both of which weaken the coulombic attraction, shift the equilibrium towards the Z form. This variation of anion geometry with cation and solvent has implications for the mechanism of anionic polymerization which will be discussed in chapter 3.

Table 6 contains chemical shift data of Li, Na, and K salts of 2-ethylpyridine in THF with and without added solvating agents at room temperature. The chemical shifts show only a slight cation dependence with the largest shift at H6

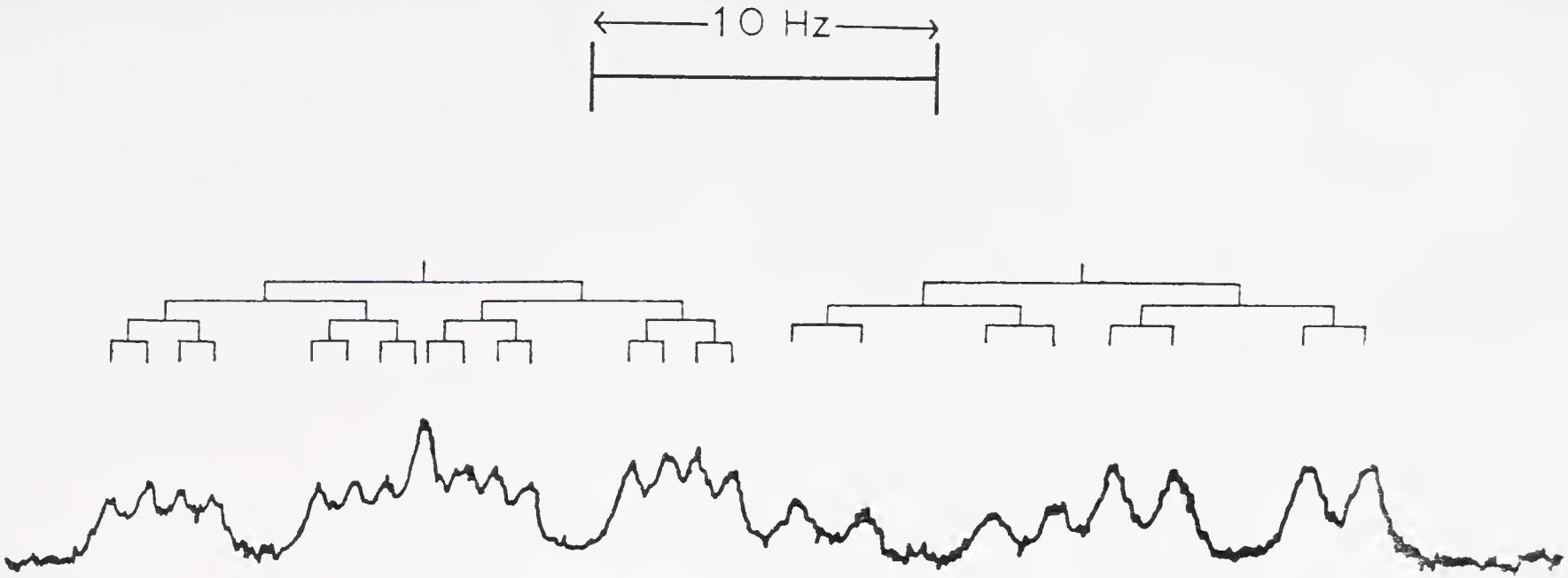

Figure 7. Expanded 60 MHz Spectrum of H4 of Li2EP in THF with [2.2.1] Cryptand Added

Table 5. Cation and Solvent Dependence of the Equilibrium between the E and Z Forms of M2EP

Cation	Solvent	E	Z	ΔG_{298} (kcal/mole)	K
Li	THF	95	5	-1.81	19.00
Li	THF/TG	82	18	-0.94	4.60
Li	THF/[2.2.1]	36	64	+0.36	0.56
Na	THF	86	14	-1.13	6.10
Na	THF/TG	66	34	-0.41	1.90
K	THF	80	20	-0.86	4.00
K[a]	NH_3	45	55	-0.12	0.82

[a]At -40°C; private communication from J.A. Zoltewicz.

Table 6. ^{1}H NMR Chemical Shifts in ppm from TMS for Li, Na, and K Salts of 2EP at 38°C

Cation	Solvent	CH_3		Hα		H3		H4		H5		H6	
		E	Z	E	Z	E	Z	E	Z	E	Z	E	Z
Li	THF	1.38	---	3.13	---	5.32	---	6.05	---	4.58	---	6.72	---
	THF/TG[a]	1.38	---	3.13	---	5.28	---	6.05	---	4.57	---	6.75	---
	THF/ [2.2.1][b]	1.37	---	3.13	---	5.18	5.37	6.03	5.68	4.50	4.28	6.78	7.02
Na	THF	1.40	1.50	3.13	---	5.32	5.40	6.15	5.75	4.68	4.55	6.85	---
	THF/TG	1.37	1.43	---	---	5.08	5.08	6.03	5.68	4.48	---	6.85	---
K	THF	1.43	1.53	3.07	---	5.27	5.35	6.15	5.78	4.67	4.63	6.97	---

[a]TG = Tetraglyme

[b][2.2.1] = [2.2.1] Cryptand

which is shifted upfield in the order K<Na<Li. The other ring positions show weaker cation dependence, with positions β, 4, and 5 showing upfield shifts with decreasing cation radius. Positions α and 3 show downfield shifts.

The effect of added solvating agents on the chemical shifts can be seen in Table 2 for the Li and Na salts. The addition of tetraglyme to the K salt produced a sparingly soluble product which was not sufficiently soluble to be studied conveniently by NMR. The addition of tetraglyme to the Na salt produced upfield shifts. The shifts were largest at positions 3 and 5. Unfortunately, the α proton was obscured by the tetraglyme absorption. The addition of tetraglyme to the Li salt resulted in very little change. However, the addition of [2.2.1] cryptand produced upfield shifts at positions 3 and 5, similar to the effect of tetraglyme on the Na salt.

The temperature dependence of the ^{1}H NMR chemical shifts of the Li, Na, and K salts is shown in Table 7. The K and Na salts show almost no temperature dependence. The Li salt however showed upfield shifts at all positions with decreasing temperature. The largest shifts were at positions 3 and 5, which are the ring carbons bearing negative charge in the resonance structures drawn for the anion.

The coupling constants for the Li, Na, and K salts are shown in Table 8. The coupling constants within the ring show no variation with cation. However, the alpha-beta coupling constant decreases in the order Li<Na<K.

Table 7. Temperature Dependence of Chemical Shift for Li, Na, and K Salts of 2EP (E isomer only) in THF (ppm from TMS)

Cation	T	CH_3	H	H3	H4	H5	H6
Li	-44°C	1.37	3.07	5.18	5.98	4.47	6.15
	6°C	1.38	3.12	5.28	6.05	4.57	6.73
	38°C	1.38	3.13	5.32	6.05	4.58	6.72
Na	-57°C	1.37	3.13	5.25	6.13	4.65	6.87
	-35°C	1.38	3.13	5.30	6.15	4.67	6.87
	38°C	1.40	3.13	5.32	6.15	4.68	6.85
	102°C	1.42	3.13	5.32	6.15	4.70	6.85
K	-35°C	1.40	3.05	5.23	6.15	4.67	7.00
	38°C	1.43	3.07	5.27	6.15	4.67	6.97
	108°C	1.43	3.07	5.28	6.15	4.67	6.95

Table 8. ^{1}H NMR Coupling Constants for 2EP Salts in THF (in Hz)

Cation	$J_{\alpha-\beta}$	J_{5-6}	J_{3-4}	J_{4-5}	J_{5-6}	$J_{4-\alpha}$	J_{4-6}
Li[a]	---	---	9.2	5.8	5.0	1.0	2.0
Li	6.4	5.5	9.0	6.0	5.0	---	---
Na	6.2	5.5	9.0	6.0	5.0	---	---
K	6.0	5.5	9.0	6.0	4.8	---	---

[a][2.2.1] Cryptand added.

High temperature studies were performed to study the interconversion between the E and Z forms. Slightly temperature dependent chemical shifts, small chemical shift differences, and unequal populations made impractical lineshape studies to determine $\Delta H^{\ddagger}$ and $\Delta S^{\ddagger}$ of the interconversion (25). However, approximate coalescence temperatures were obtainable, providing information concerning cation and solvent effects upon the rotational barrier. The coalescence of the methyl peak of Na2EP is shown in Figure 8. The results of the studies are shown in Table 9. The barrier increases in the order Li<Na<K. The Li salt was studied only with tetraglyme added, because in THF alone the Z form was not present in a sufficiently large quantity. Addition of tetraglyme to the Na salt lowered the barrier. An attempt to see if addition of [2.2.2] cryptand would further lower the barrier for the Li salt failed due to the rapid decomposition of the sample.

The high barrier to rotation suggested the possibility of measuring the rate constant for interconversion at low temperatures by perturbing the system and observing the relaxation to the new equilibrium populations. The experiment was performed by adding [2.2.1] cryptand to the Li salt in THF at -78°C. The first ^{1}H NMR spectrum, approximately 20 minutes after the addition, showed that the system had already achieved the new equilibrium value. Although a rate constant could not be measured, the experiment does allow a lower limit to be put on the rate constant. The kinetic treatment for a system perturbed from equilibrium produces Equation 4 where c_i is the concentration at time t, $\bar{c}_i$ is

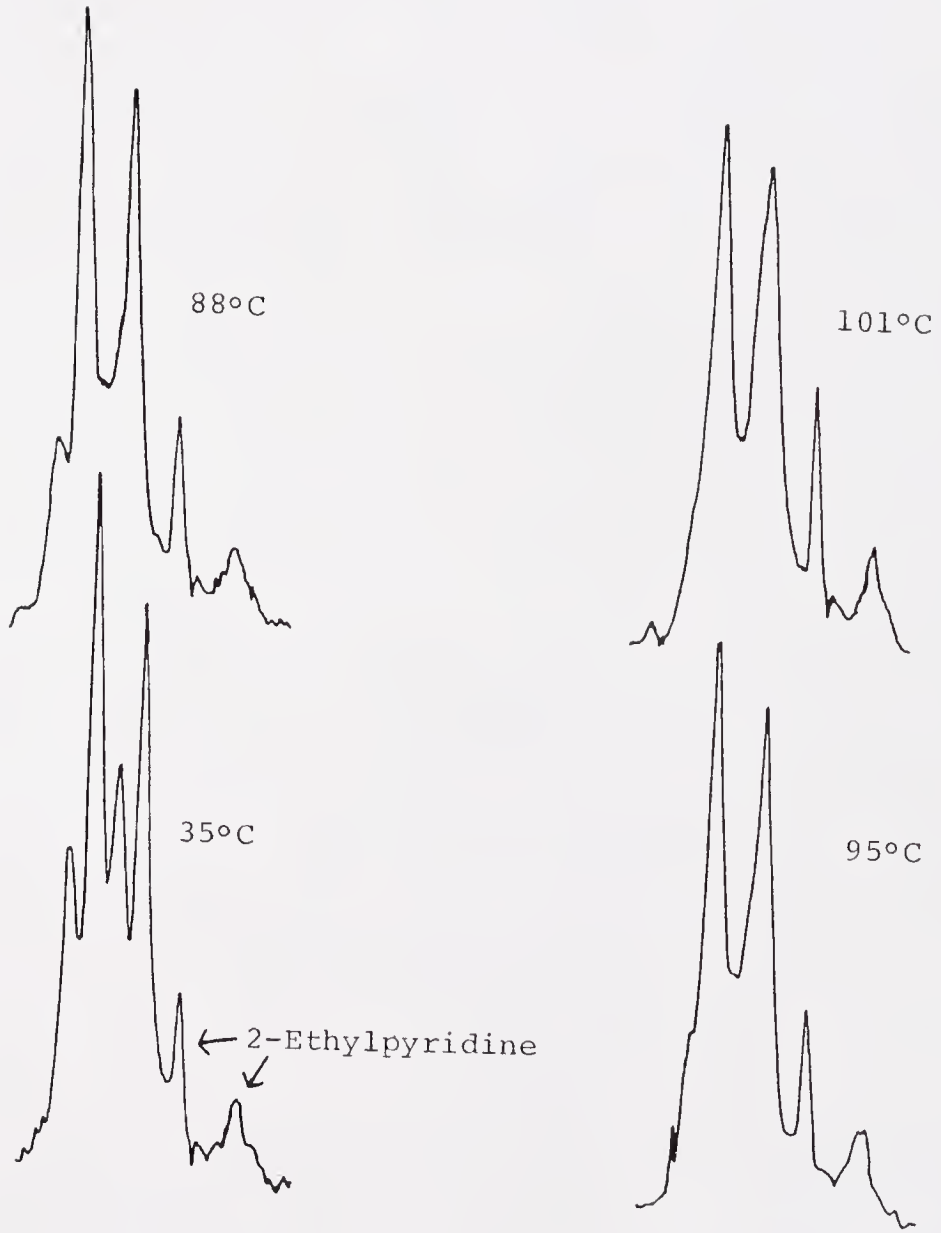

Figure 8. Coalescence of the Methyl Peak of Na2EP in THF/TG

Table 9. Coalescence Temperatures and Free Energy Barriers for the Equilibrium between E and Z Forms of M2EP Salts

Cation	Solvent	Coalescence Temperature	$\Delta G^{\ddagger}_{E\rightarrow Z}$ [a] (kcal/mole)
Li	Tetraglyme	65°C	18.7
Na	THF	105°C	20.3
Na	THF/Tetraglyme	95°C	20.6
K	THF	>120°C	>22

[a] Determined from the equation $\Delta G^{\ddagger}_{E\rightarrow Z} = RT_c(\ln[kT_c/h] - \ln k_{E\rightarrow Z})$; $k_{E\rightarrow Z}$ at coalescence temperature calculated from the relationship $\tau = 1/[\sqrt{2}\pi(\delta\nu)]$

$$\frac{(c_i - \bar{c}_i)}{(c_{i,0} - \bar{c}_i)} = \frac{-t}{e^{\tau}}$$

Equation 4

the concentration at equilibrium, τ is the time required for the perturbation to relax to 1/e of its original value, and $c_{i,0}$ is the concentration immediately after the perturbation (26). The results show $k \geq 7 \times 10^{-4} s^{-1}$ at -60°C.

The ^{13}C - ^{1}H coupling constants for Li and Na2EP are given in Table 10 together with those of pyridine (27). All of the ring coupling constants either agree with those of pyridine or are smaller in agreement with the relation that increased negative charge density reduces the magnitude of ^{13}C - ^{1}H coupling (28).

The ^{1}H NMR spectra of the Li and Na salts of 1,3-di-2-pyridylbutane were observed in THF and are shown in Figure 9. The spectra were observed without recrystallization of the salts because spectra after recrystallization indicated the occurrence of undesirable reactions. Therefore, the spectra were not taken in d_8-THF and only the region in which H4 and H3 are found was suitable for study. Even these absorptions were not easily analyzed in the same manner as the 2-ethylpyridyl anion spectra. The Na salt possesses the simpler spectrum. The observed spectrum seems to indicate that the E/Z ratio is much lower than in Na2EP, approximately 55% E and 45% Z.

^{13}C NMR Results

The ^{13}C NMR spectra of the Li, Na, and K salts are summarized in Table 11. The order of the chemical shifts is the

Table 10. ^{13}C-^{1}H Coupling Constants (in Hz) of M2EP Salts in THF

Compound	Cβ	Cα	C3	C4	C5	C6
Li2EP	125	147	156	150	163	162
Na2EP	122	146	154	150	160	159
Pyridine			163	152	163	170

a)

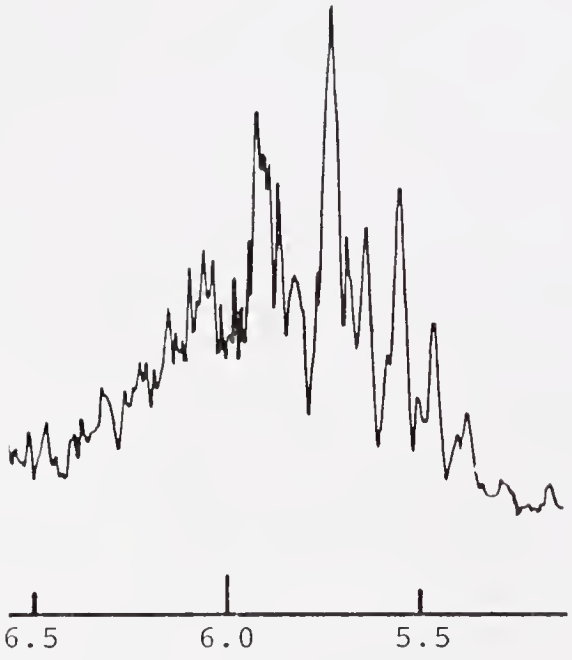

b)

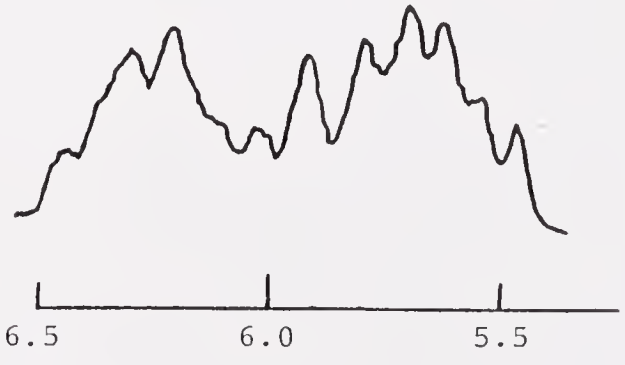

Figure 9. ^{1}H NMR Spectra of Li and Na Salts of the 1,3-Di-(2-pyridyl)butane Anion. a) 100 MHz Spectrum of Li Salt. b) 60 MHz Spectrum of Na Salt. (Chemical shifts in ppm from TMS)

Table 11. ^{13}C NMR Chemical Shifts of Li, Na, and K Salts of 2EP in THF (ppm from TMS)

	Cβ		Cα		C2		C3		C4		C5		C6	
Cation	E	Z	E	Z	E	Z	E	Z	E	Z	E	Z	E	Z
Li	13.5	--	68.4	--	156.7	--	110.3	118.9	132.5	128.5	94.9	94.7	150.4	149.8
Na	13.6	--	65.9	--	157.6	--	109.2	126.8	133.5	130.4	95.6	95.4	151.5	150.8
K	14.1	--	67.1	--	157.8	--	108.3	116.8	133.3	130.4	94.7	94.4	151.4	151.0

same as for the ^{1}H NMR spectra. The presence of both rotameric forms is evident in all spectra, including that of Li salt. The C2 absorbance was assigned from a coupled ^{13}C NMR spectrum which also confirmed the location of the Cα resonance within the downfield d_8-THF signal (and permitted the assignment of C2). The ^{13}C NMR spectra are useful in studying the charge distribution within the anion because anisotropic effects are less important in relative terms than for ^{1}H NMR (28,29). Also, since C2 can be observed, ^{13}C NMR provides information about every position except nitrogen.

CNDO/2 Calculations

Semiempirical and ab initio molecular orbital calculations have been used quite extensively to study ion pair structure, especially the nature of the carbon-lithium bond (30-33). In alkyllithiums, the calculations support the concept of prevalent covalent character. In the case of delocalized systems the organolithium compound appears to exist as either an undissociated ion pair or as a dissociated ionic salt, and these experimental results have also been supported by the results of ab initio and semiempirical calculations (30-33).

The CNDO/2 method which was selected for this study has been widely used and its strengths and weaknesses are well known (34). It is qualitatively good at predicting stable geometries with errors in bond length of about 0.1 Å and bond angles of a few degrees. The calculated atomic charges are usually good to within a few hundredths of an electron. The stability of compact geometries is somewhat overestimated.

Calculations were performed to find the optimum position of the cation, the charge distribution in the anion, the hybridization of Cα, and the bond order of the Cα-C2 bond.

The calculations were begun on the picolyl system using bond angles and bond lengths reported for the pyridine ring (35). The Cα-C2 bond length was first optimized in the free anion, assuming an sp^2 hybridization at Cα. The position of Li was then optimized for positions both in the nodal plane and above the delocalized carbanion. The hybridization at Cα was also varied to compare the energies of a delocalized anion and a "covalent" species with sp^3 hybridization at Cα. The position of the cation is important in order to make a distinction between structures:

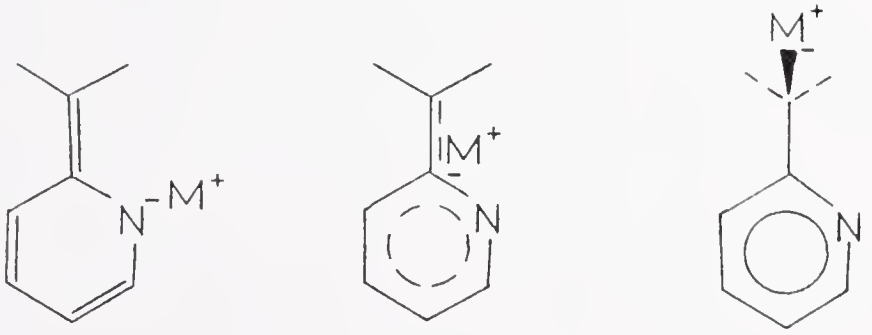

The calculations indicate that the cation should be located above the plane of an sp^2 hybridized anion. Figure 10 shows the contour map for various cation positions at a height of 2.0 Å above the plane. The potential well is shallowest along the line which represents points 2/3 as far from the nitrogen as from Cα. The potential well is much steeper as the cation is displaced towards either Cα or nitrogen. The optimum position for the cation in the nodal plane is calculated to be approximately 60 kcal/mole higher in energy and thus

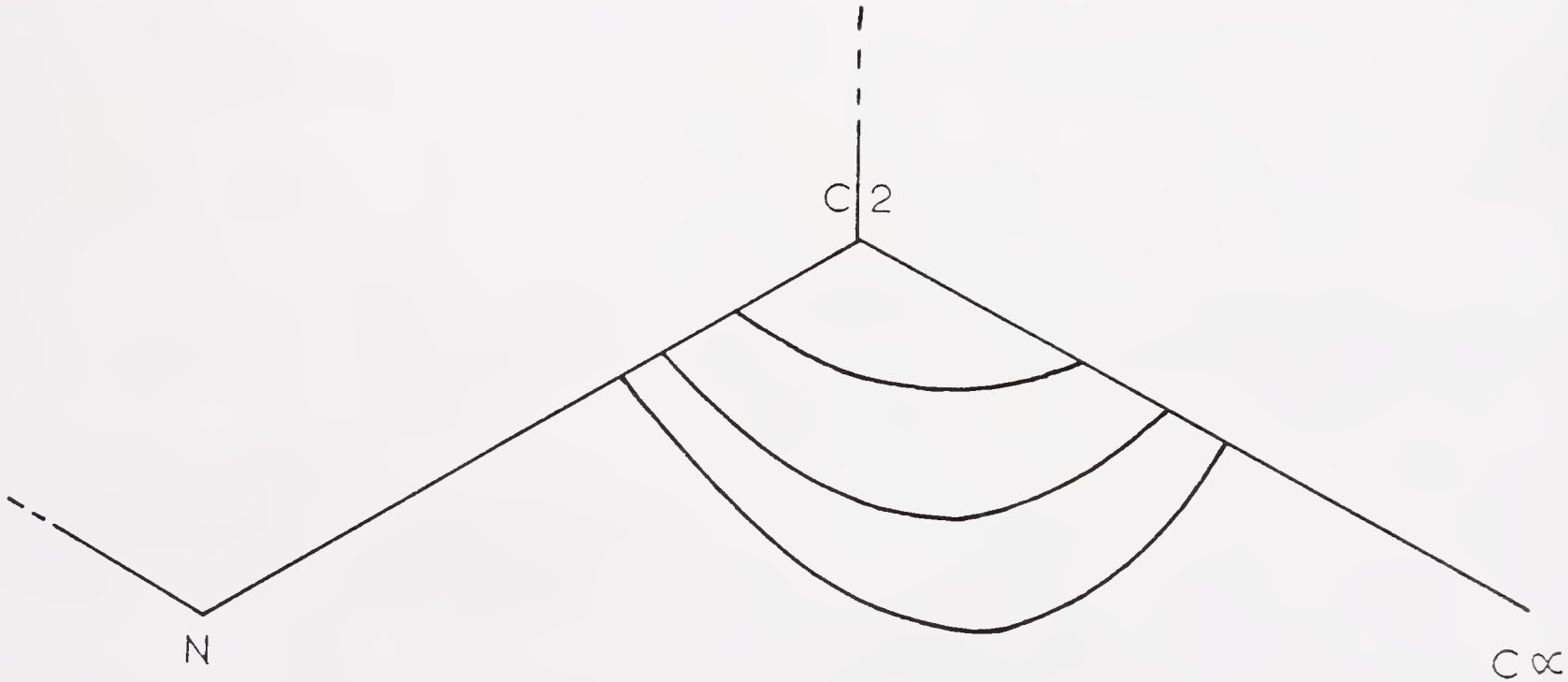

Figure 10. Energy Contour Map for Variation of Li Position at 2.0 Å Above the Plane of the 2-Picolyl Anion: a) +0.05 hartree b) +0.10 hartree c) +0.15 hartree

can be excluded. These results are in reasonable agreement with the findings of Bougini et al. (30) who performed ab initio calculations on the allyllithium system and of Eizner and Erussalimsky who carried out CNDO/2 calculations on a variety of models for propagating anionic species (32). Of course, these calculations pertain to the ion-pair in the gas phase. However, calculations which have included solvation of the cation (water molecules or dimethyl ethyl) have shown that the effect of solvation continues to favor the relative stability of the cation above the plane (30,33). Since coordination of the cation at a position in the nodal plane adjacent to the methylene could result in steric problems calculations were also executed with the methylene unit twisted out of plane. The results indicated that the loss of overlap with the ring was much more costly than the benefits derived from lessening of steric repulsions and improved overlap between the Cα and the Li orbitals.

The charge distribution which was calculated is shown in Figure 11. The bulk of the negative charge is located at Cα and nitrogen, resulting in a charge distribution similar to an allylic system. This observation is interesting in view of the fact that the dissociation constant of the sodium salt of living poly-(2-vinylpyridine) ($K_d = 0.87 \times 10^{-9}$) is much closer to that of living poly-(butadiene) ($K_d \sim 10^{-9}$) and living poly-(methylmethacrylate) ($K_d = 0.44 \times 10^{-9}$ for Li salt) than to living polystyrene ($K_d = 1.5 \times 10^{-7}$) (2).

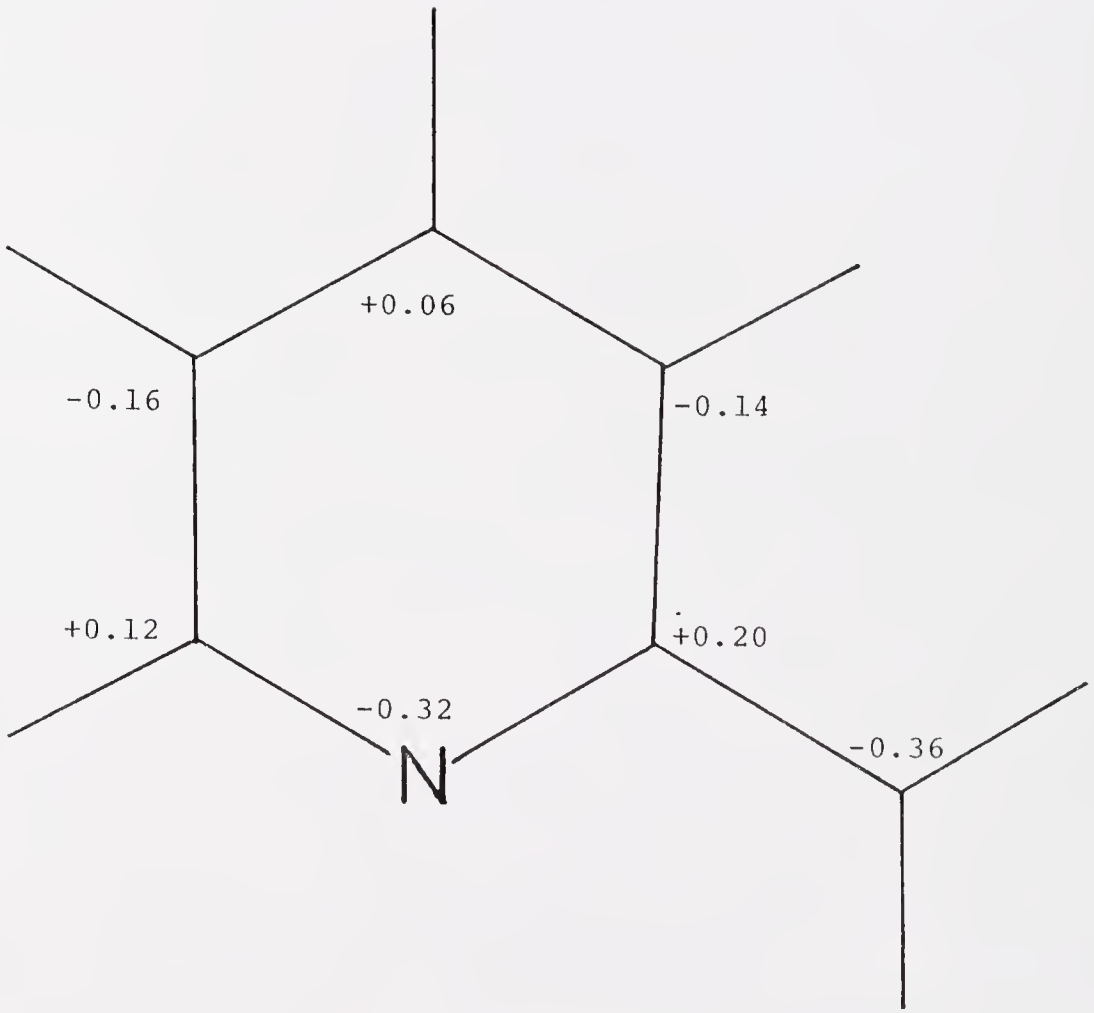

Figure 11. Calculated Charge Densities for 2-Picolyl Anion

Calculations were also carried out for the 2-ethylpyridyl anion. The optimum conformation of the methyl group was determined for both E and Z forms by calculations on the free anion. The energy difference between the E and Z isomers was found to be very slight, with the Z isomer being favored by 0.14 kcal/mole. The small difference in energy between the two isomers is in agreement with the findings through ^{1}H and ^{13}C NMR for systems where the cation is powerfully solvated The E iosmer is actually favored in tight ion pairs and the trend observed with change in cation size is opposite from that calculated. However, the differences between the calculations and experimental results are relatively small and may be explained by the effect of solvation, possibly resulting in a slightly different cation position, or steric repulsions between the solvation shell and the methyl group which were not included in the CNDO calculations.

CNDO/2 calculations were also used to investigate the barrier to rotation. As a model for the transition state the calculations were performed for the free anion corresponding to a 90° rotation of the methylene group. The calculated rotational barrier for the 2-picolyl anion is 1.9 kcal/mole greater than that for the benzyl anion. This is reasonable since the nitrogen pulls a greater amount of charge into the ring, increasing the double bond character between the alpha carbon and the ring. If the difference in rotational barriers were entirely due to differences in delocalization energy, then the difference in pK_a values between toluene and 2-picoline could be used to arrive at a value for

the difference in rotational barriers. This approach, using pK_a's of 31 and 35 for 2-picoline (36) and toluene (37) respectively, predicts the barrier for the 2-picolyl anion to be 5.0 kcal/mole higher than the benzyl anion. However, in evaluating this estimate it is important to recognize that the pK_a's are for two systems in which the ion pairing and solvent effects may be quite different.

The calculated barriers of rotation of 35.9 kcal/mole for the 2-picolyl anion and 34.0 kcal/mole for the benzyl anion are extremely high. This may in part be due to one of the problems with CNDO/2 calculations in that they tend to overemphasize the effect of overlap (38).

The calculated π bond orders for the 2-picolyl anion are shown in Figure 12. The bond orders for the 2-picolyl anion clearly show the importance of the resonance form placing charge on nitrogen and double bond character between C2 and Cα.

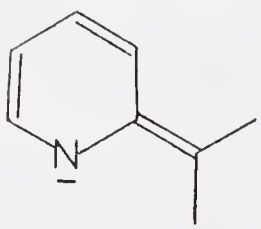

Discussion

A full description of ion pair structure requires discussion of charge distribution in the anion, anion geometry including hybridization of the alpha carbon, cation position, and the tightness of the ion pair. The results from UV/conductance studies, ^{1}H and ^{13}C NMR, and CNDO/2 calculations all provide information about the various aspects of ion pair structure.

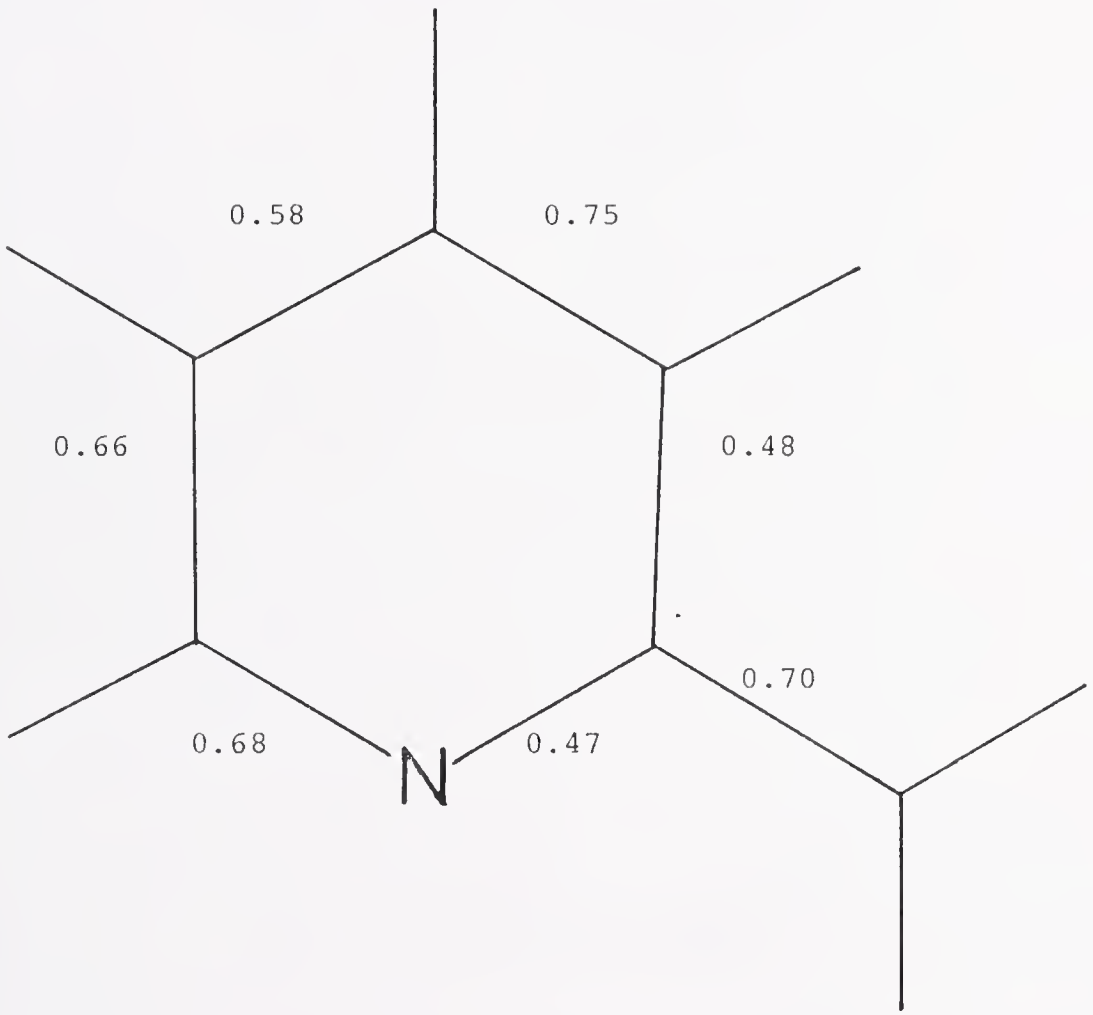

Figure 12. Calculated π Bond Orders for the 2-Picolyl Anion

"Tightness" of the Ion Pair

The conductance data indicate the 2-alkylpyridyl salts to exist as very tight ion pairs, tighter than the 2-pyridylphenylethylene salts which exist as tight ion pairs even at -75°C (39). Only with the addition of [2.2.2] cryptand was there evidence for the formation of a loose $2EP^-$ ion pair. The very low K_d values for the Na salts of 2EP and 1,3-DPB are expected on the basis of the reported K_d for living poly-(2-VP)Na of 0.87×10^{-9} (11,40). Addition of dibenzo-18-crown-6 increases the K_d but has no effect upon the UV spectrum. This behavior is typical of a peripherally solvated contact ion pair (41). Addition of [2.2.2] cryptand also introduces a red shift of 8 nm. Red shifts in the UV are associated with a significantly decreased cation-anion interaction and are usually observed in the conversion from a tight to a loose ion pair (41).

The deviations from a linear Kraus-Brey plot at concentrations greater than 10^{-3} M and the excellent fit for the triple ion plot indicated the formation of triple ions at high salt concentrations for both Na2EP and DPB. However, even in a 1 M solution the estimated proportion of triple ions is less than 3%.

Charge Distribution

The relationship between charge delocalization and the tightness of ion pairs suggests that the charge in 2EP carbanions is less delocalized than that in the analogous carbon compounds. The similarity of the dissociation constant to those of living poly(butadiene) and poly(methylmethacrylate)

as discussed earlier implies that the charge in fact may reside primarily on the alpha carbon and nitrogen. Such a charge distribution was used earlier to explain the tightness of the 2- and 4-pyridylphenylethylene salts compared to the 3-pyridylphenylethylene salts (39).

Calculations performed on the 2-picolyl anion predicted the charge distribution shown in Figure 10 with approximately 2/3 of the negative charge localized on the nitrogen and the alpha carbon. Considering that the presence of a cation should further polarize the anion, it appears that 2-alkylpyridyl carbanions are essentially ambident anions, with some delocalization onto carbons 3 and 5.

Negative charge density is associated with upfield shifts in both ^{1}H and ^{13}C NMR (42). The ^{13}C NMR technique is considered more reliable for determination of charge densities because anisotropy plays a less important role in determining chemical shifts (28,29). Charge densities may be calculated by measuring upfield shifts relative to a model compound and multiplying by 160 ppm per electron for ^{13}C NMR (28,43-45). The model compound for $2EP^-$ salt would logically be 2EP. However, the alpha carbon presents a problem because in 2EP it is sp^3 hybridized, but in $2EP^-$ it appears to be sp^2 hybridized as will be discussed later. To take into account the effect of the change in hybridization, the model chosen for Cα was 2-vinylpyridine. The results are compared in Table 12 with CNDO/2 calculations for the change in charge distribution between 2-picoline and 2-picolyl anion. The

Table 12. Comparison of Charge Densities Calculated from ^{13}C NMR with CNDO/2 Calculations

	Cα	C2	C3	C4	C5	C6
^{13}C NMR[a]	-0.346	0.00	-0.09	-0.03	-0.18	0.00
CNDO/2[b]	-0.34	+0.06	-0.09	+0.01	-0.12	+0.02

[a]Calculated by multiplying the difference in shift between the 2-ethylpyridyl anion and the neutral model compound (2-ethylpyridine for the ring carbons; 2-vinylpyridine for Cα).

[b]Difference in calculated charge densities of 2-picoline and the 2-picolyl anion.

agreement is satisfactory, and indicates that the calculated charge distribution is a reasonable estimate.

^{1}H NMR studies of alkali metal salts of 1- and 2-methylnaphthalenes (46) revealed systematic variations in chemical shifts as a function of cation radius, which were explained in terms of increasing polarization of the anion towards the Cα with smaller cations. The chemical shifts tabulated in Tables 6 and 11 for M2EP salts do not reveal such cation effects. This may be an indication that the cation is not as closely associated with Cα in $2EP^{-}$ salts as in the methylnaphthyl salts.

A change in the solvation of the cation should likewise affect the charge distribution. Although ^{13}C NMR spectra are not available, the ^{1}H NMR spectra of Li and Na salts of 2EP described in Table 6 show significant upfield shifts at H3 and H5 with the addition of the cation solvating agents tetraglyme and [2.2.1] cryptand. The Li salt showed only small upfield shifts with the addition of tetraglyme, but the addition of [2.2.1] cryptand produced rather large shifts. The shift of Cα could not be studied due to absorptions of the tetraglyme and the [2.2.1] cryptand. Thus, increasing cation solvation appears to result in less polarization of the anion by the cation.

Similarly, as solvation increases at lower temperatures, H3 and H5 would be expected to experience upfield shifts. In accordance with this prediction, the Li salt, for which peripheral solvation should be the most important due to its small size, shows the greatest temperature dependence.

Although upfield shifts occur at all positions, H3 and H5 do show the largest change. However, the shifts are much less than those associated with addition of solvating agent.

Cation Position

The charge distribution as discussed in the preceding section suggests that the cation should be located at a position intermediate between the alpha carbon and nitrogen. However, the questions remain of whether the cation is located above the plane or in the plane of the anion and whether the cation is more closely associated with carbon or nitrogen.

The observation of two isomeric forms indicates a planar or near planar structure. Thus, if the cation were located in the nodal plane, as shown, the cation would suffer peri

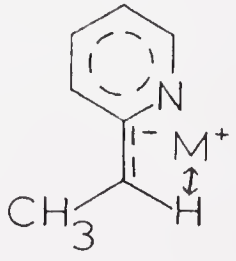

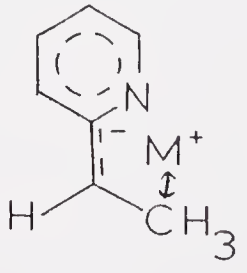

interactions with the alpha proton in the E isomer and the methyl group in the Z form. Consideration of the additional steric constraints of the solvation shell makes this position appear even less favorable. Also, this position places the cation at a large distance from the alpha carbon which should still bear a large portion of the charge.

A position above the plane but intermediate between nitrogen and the alpha carbon is more reasonable in order to maximize coulombic attractions. Such a position also allows coordination of solvent with less steric interference.

Calculations performed on the Li salt of 2-picoline show the above plane position which allows overlap between a p orbital of Li and the HOMO of the 2-picolyl anion as shown in Figure 13 to be much preferred over a nodal-plane position.

These findings correlate with ^{1}H and ^{7}Li NMR investigations of fluorenyl salts which demonstrated the cation to be above the ring as determined by upfield shifts of the Li and the cation solvating agents complexed to the cation (47, 48). Likewise, a similar allylic-type position was suggested for Li salts of 1- and 2-methylnaphthalenes (46). Furthermore, in crystals of benzyllithium ethylenediamine, the Li is coordinated in an allylic manner (49). Thus, it seems that the anion is capable of competing with the solvent for a second coordination site. This type of structure has also been shown to be favored in a number of CNDO/2 studies of Li salts of compounds with allylic-type charge distributions (30-33).

Anion Geometry

The observation of two isomeric forms in ^{1}H NMR and ^{13}C NMR spectra is indicative of double bond character about the C2-Cα bond, and significant sp^2 character at Cα. The magnitude of ^{13}C-^{1}H coupling is related to the s character at carbon. Although this relationship has been abused when other factors have been ignored, it remains useful (28). The ^{13}C-^{1}H coupling constant of 149 Hz at Cα is well above that expected for sp^3 hybridized carbon, especially considering that negative charge decreases the coupling as in the comparison of 125 Hz for methane and 98 Hz for methyllithium

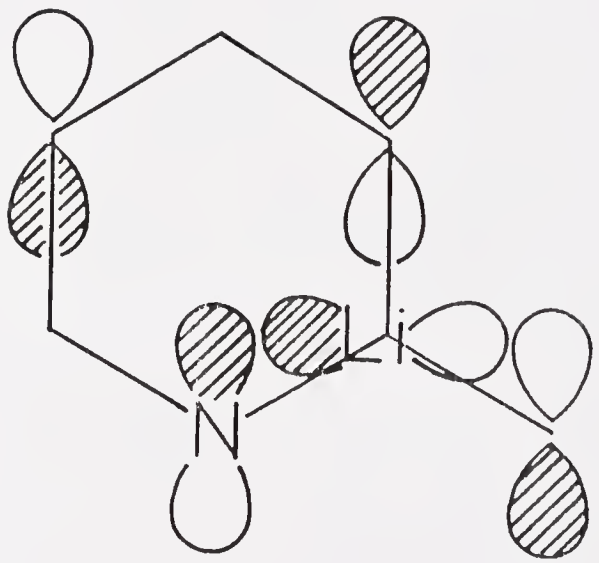

Figure 13. Overlap of Li p Orbital with the HOMO of the 2-Picolyl Anion

(50). In fact, the ^{13}C-^{1}H coupling constant is close to those of the ring carbons. These findings are in agreement with the predictions from the geminal coupling constants reported in 2-picolyl salts (24) and 1- and 2-methylnaphthalene salts (46), which also indicated sp^2 hybridization for Cα.

The equilibrium between the diastereomers E and Z shows an interesting dependence on cation and solvent as shown in Table 5 on page 24. The results of calculations are of little assistance in studying this problem. They predict the Z isomer to be more stable for the free ion, and favored more with decreasing cation size, the opposite of the observed trend.

Increasing cation size and cation coordination increases the proportion of the Z isomer. From the UV/conductance studies it appears that tetraglyme and dibenzo-18-crown-6 externally complex the cation. Such complexation, although not leading to separated ion pairs, does result in a loosening of the contact ion pair. The distance separating the ions is increased, thereby lessening steric crowding. Another factor to be considered is that the solvating agent may simply coordinate in such a way as to be less sterically demanding than the solvation shell of THF molecules. The addition of [2.2.1] cryptand to the Li salt apparently forms a separated ion pair in view of the UV/conductance findings for the [2.2.2] complexed Na salt. The Li salt with [2.2.1] and K in liquid NH_3 may resemble the free ion and were the only two systems to show a preference for the Z isomer, which according to CNDO/2 calculations is preferred for the free anion.

The trends observed are the same as those reported for the 2-alkenyl salts shown in Table 13 (51). For each alkenyl salt the Z/E ration increases with cation radius and increased cation solvating power. As the alkyl group attached to the allylic anion becomes larger, the Z/E ratio decreases. As in the present study however, the free anion appears to prefer the Z configuration. Explanations for this preference include a hyperconjugative interaction as shown on the left. The MO

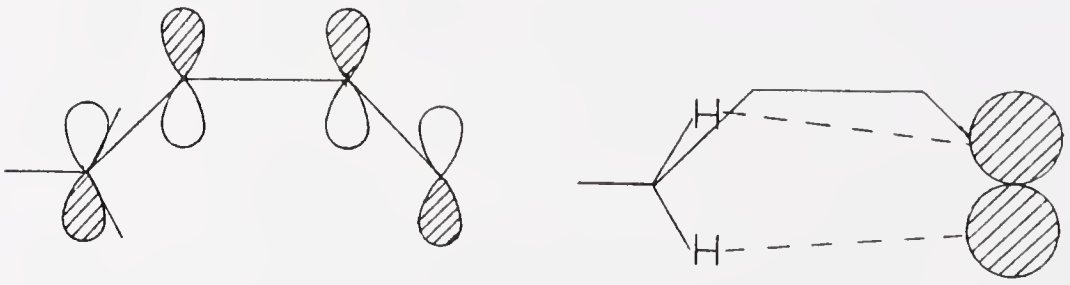

drawn is the highest occupied MO for a delocalized 6 π-system. Thus attractive forces between the alkyl groups and the negatively charged methylene terminus could explain the Z preference. The alternative explanation which the authors preferred was hydrogen bonding between the alkyl groups and the electron-rich terminus. Both suggestions are possible in the $2EP^-$ system, assuming that such attractions are more powerful for the more negatively charged N than for C3.

The absence of temperature effects on the equilibrium between the E and Z isomers indicates that $\Delta H \simeq 0$ for the interconversion between the two anion geometries. This means that variations with cation and solvent must be explained on the basis of entropy considerations. Thus the effect of the steric repulsions between the solvation shell of the cation

Table 13. Z/E Equilibrium Composition of 2-Alkenylmetallic Compounds RCH = $CHCH_2M$ in Hexane Solution or Suspension (in parentheses: in THF), as Reflected by the Z/E Isomeric Composition of Derivatives Obtained by Quenching with Oxirane

	M = H	M = MgBr	M = Li	M = Na	M = K	M = Cs
R = CH_3	23:77	54:46	67:33 (85:15)	93:7	96:4 (99.2:0.8)	99.9:0.1
R = CH_2CH_3	29:71	39:61	24:76 (80:20)	61:39 (85:15)	94:6	90:10
R = $CH(CH_3)_2$	26.74	23:77	14:86	38:62	56:44 (78:22)	66.34
R = $C(CH_3)_3$	0.1:99.9	0.2:99.9	3:97 (4:96)	7:93 (8:92)	8:92 (13:87)	9:91 (12:88)

M. Schlosser and J. Hartmann, J. Am. Chem. Soc., 98, 4674 (1976).

and the methyl group leads to restrictions of the rotation of the methyl group and the rotation of the solvent molecules coordinated to the cation. This explanation also indicates that the cation must be located off the axis of the C2-Cα bond. This explanation seems reasonable for a system where the steric crowding is not severe. As steric crowding increases, in general the first effect should be one of restricting freedom of movement in situations where multiple conformations are of similar energy. As steric bulk further increases, eventually a point should be reached where none of the original lowest energy conformations are accessible, and steric crowding begins to produce an enthalpy effect as bond angles and bond distances are distorted to obtain the lowest energy conformation. In the $2EP^{-}M^{+}$ system, it appears that the Z isomer is favored for the free anion, but the presence of a cation with its solvation shell produces entropy effects which lead to a favoring of the E isomer.

Kinetics of Isomerization

The kinetics of the isomerization between the E and the Z isomers was investigated by high temperature ^{1}H NMR. Although quantitative results were not obtained owing to the difficulties inherent in the system, coalescence phenomena were observed as shown in Figure 8, and the effect of cation and solvating agent was studied. The order of coalescence temperatures indicates the barrier to rotation to be greatest for K and least for Li. The addition of tetraglyme to the Na salt produced a slight lowering of the barrier.

Dynamic studies of similar processes in the 1- and 2-methylnaphthalene (46) and phenylallyl carbanions (52) show a similar trend with cation size.

The rotation may occur either as rotation within a delocalized anion or by way of a small concentration of a covalent species as suggested by Bates et al.(53) and shown in Equation 5.

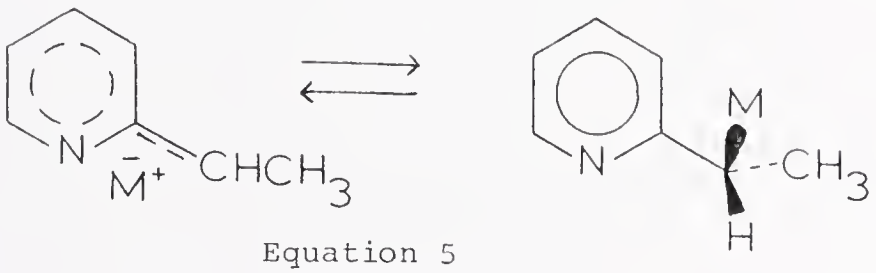

Equation 5

Kronzer and Sandel preferred to explain their results for the effect of cation on rotation in the methylnaphthalene carbanions on the basis of increasing covalency with decrease in cation size (46). An increase in covalency of the cation-anion bond should lower the C2-Cα π bond order and reduce the rotation barrier.

In the $2EP^-$ ion pairs it might be expected that a smaller cation would polarize the anion towards nitrogen, reducing charge from Cα, and thereby increasing the bond order at C2-Cα. However, the observed order of rotational barriers indicates that this is not the case.

CHAPTER III

BETA-CARBON STEREOCHEMISTRY

Results

Although for a simple vinyl monomer beta-carbon stereochemistry is undefined, an understanding of the beta-carbon stereochemistry of beta-deuterated monomer is required in order to completely understand the polymerization process. In this chapter, results of experiments investigating the effects of cation, solvation, monomer structure, and degree of oligomerization in the anionic oligomerization of 2-vinylpyridine will be presented.

Monomers Used

The deuterated monomers [4], [5], and [6] required were prepared as discussed in Chapter IV.

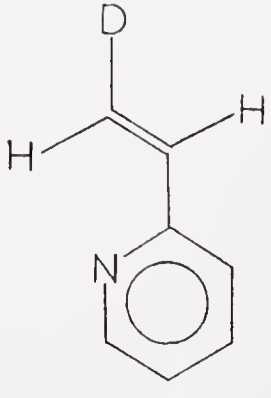

[4]

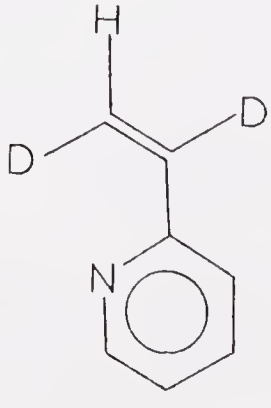

[5]

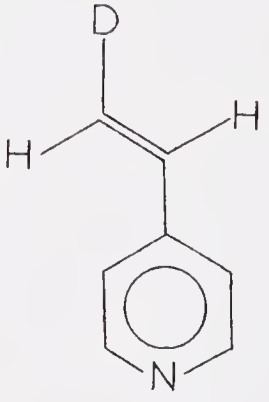

[6]

Assignment of Beta-Protons

In the ^{1}H NMR spectra of the oligomers of 2-vinylpyridine prepared as discussed in Chapter I, the question arises as to which position is the erythro proton and which is the threo. Although a conclusive assignment cannot be made at the present

time, there are some indications that the downfield position is probably the erythro and the upfield the threo. Studies in both meso-dichloropentane (54) and meso-dicarbomethoxy-pentane (55) have indicated that the coupling with the alpha-protons is usually greater for the erythro than the threo in agreement with arguments made on the basis of preferred conformations. In meso-2,4,di-(2-pyridyl)pentane the corresponding coupling constants are 7.5 Hz for the downfield and 6.5 Hz for the upfield position. In the conformations found to be prevalent for meso-disubstituted pentanes (13), it appears that the erythro proton should be in a deshielding region with respect to the pyridine ring. An unequivocal assignment in the meso-dicarbomethoxy pentane (55) has demonstrated the erythro proton is more likely to be the one downfield, and the remainder of the discussion in this dissertation will assume the above assignment to be correct.

Cation Effects

The dimeric products with Li and K as counterions were prepared as shown in Equations 6 and 7. D_2O was used instead

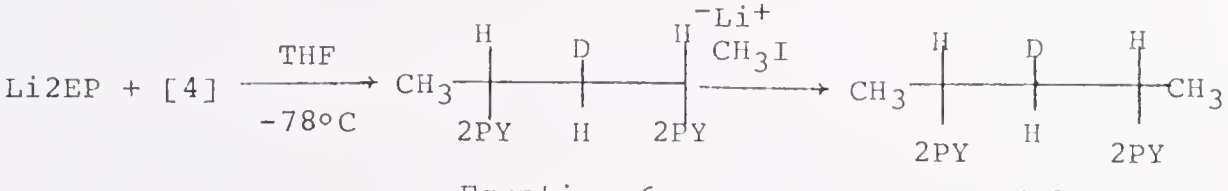

Equation 6 [7]

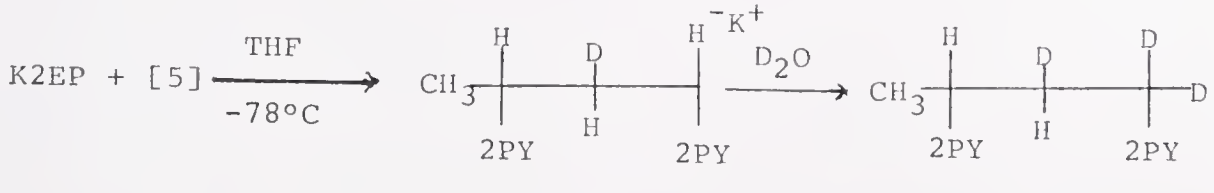

Equation 7 [8]

of CH_3I in Equation 7 to avoid the formation of racemic pentane (see Table 1). Since it was known that the difference in chemical shifts of the beta methylene protons in 1,3-di-(2-pyridyl)butane is very small (20), monomer [5] was used to reduce the coupling and enhance the probability of being able to resolve the signals. As it turned out, the signals still overlapped in the 100 MHz spectrum, but the 270 MHz spectrum easily resolved the two absorptions. The 60 MHz ^1H NMR spectrum of [7] is shown in Figure 14 and the 270 MHz ^1H NMR spectrum of [8] is shown in Figure 15. Keeping in mind that the monomers differed in the placement of deuterium, the large downfield absorption for [7] and the large upfield absorption for [8] indicate that the preferred mode of presentation is the same in both cases, assuming the relative chemical shifts of the erythro and threo positions are unchanged. After correcting for the monomer composition, selectivity with Li was 91% and with K the selectivity was 77% as shown in Table 14. Thus an increase in cation size reduces the selectivity of beta-carbon stereochemistry in a manner very similar to the reduction in preference of the E isomer of $2EP^-$.

Solvation Effects

To investigate the effect of increased cation solvation the oligomerization was carried out in a THF solution with 2.5 equivalents of tetraglyme added after the formation of Li2EP. The stereochemistry was the same within experimental error as for the reaction carried out in THF alone.

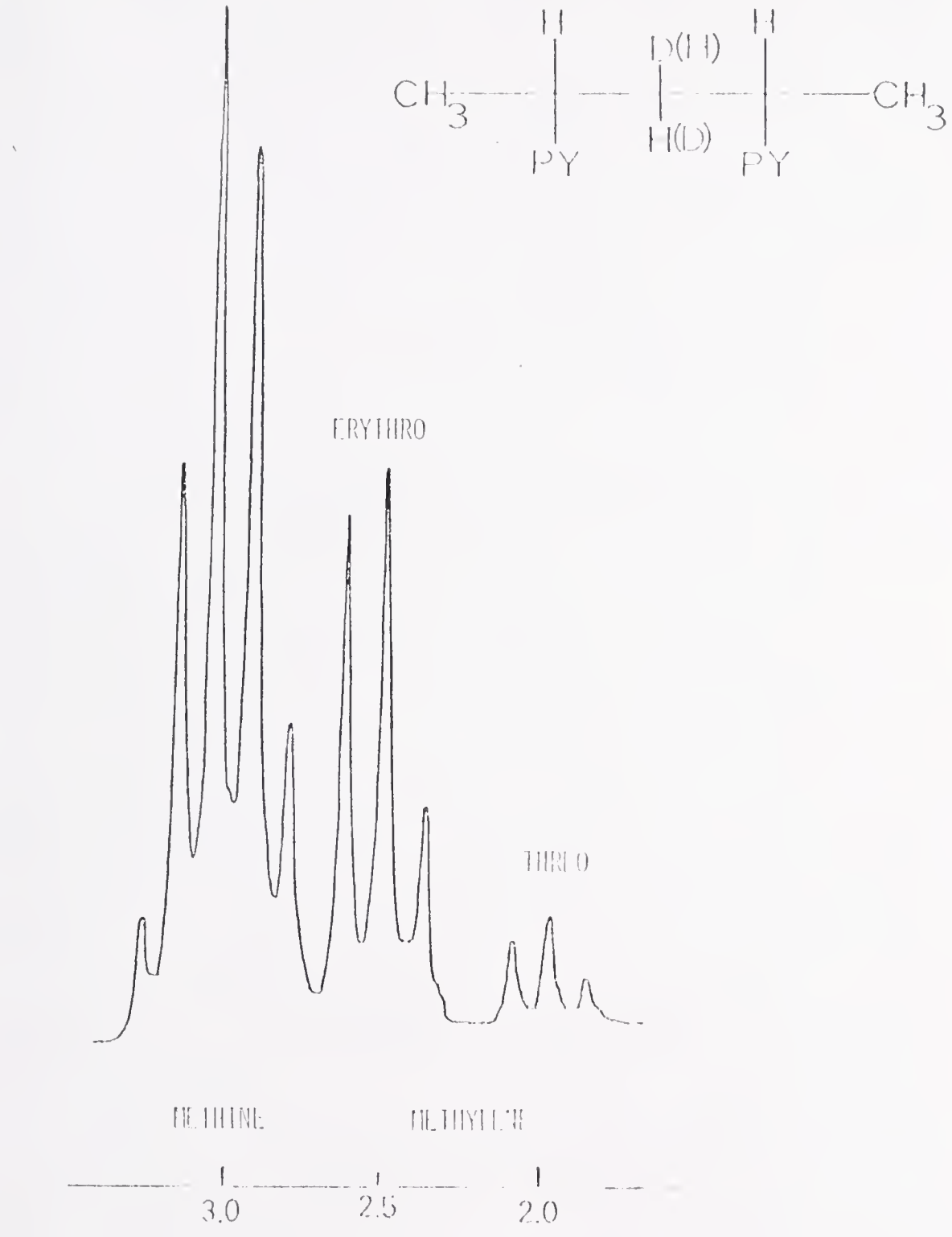

Figure 14. 60 MHz ^{1}H NMR Spectrum of [7]

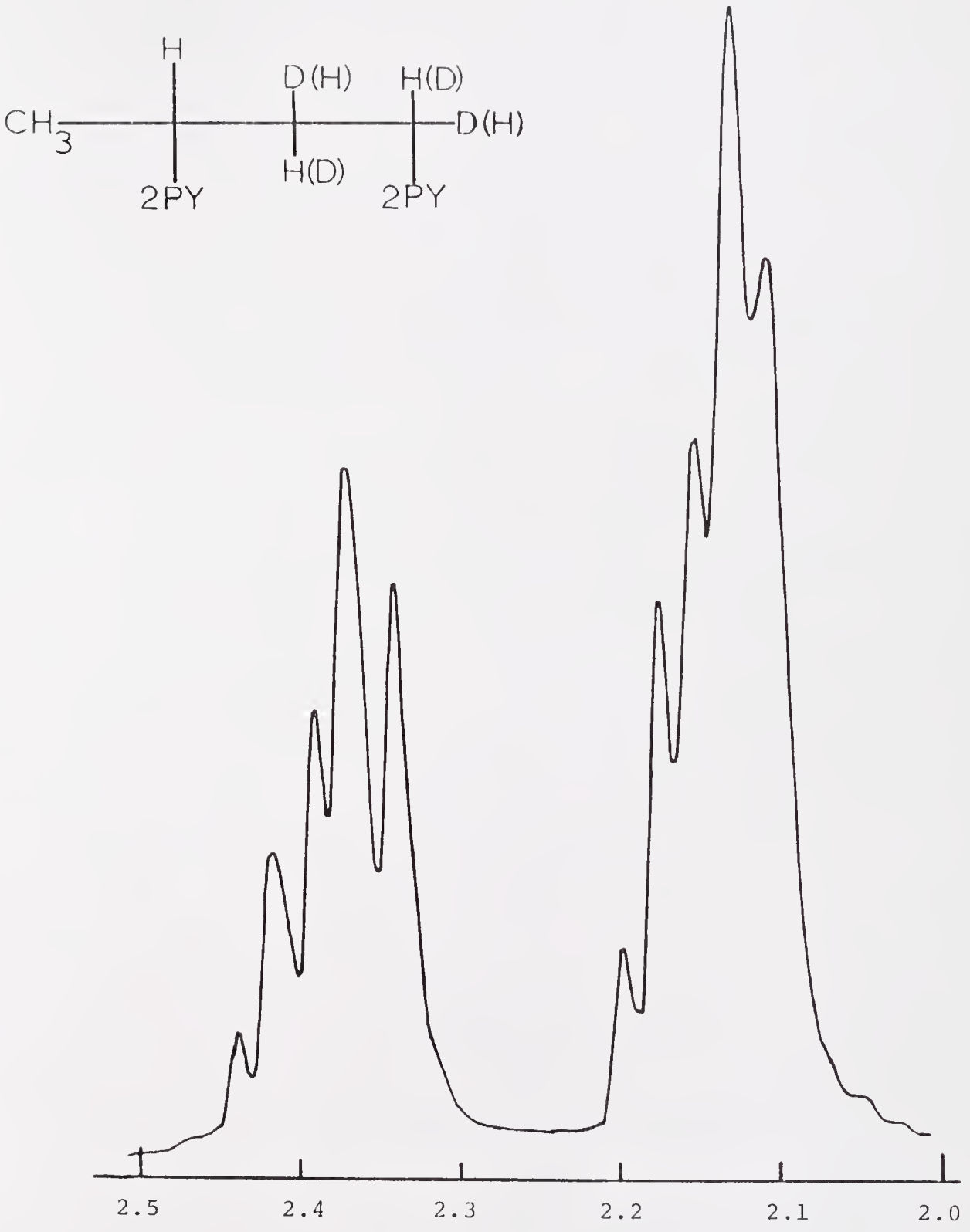

Figure 15. 270 MHz ^{1}H NMR Spectrum of [8]

Table 14. Beta-Carbon Stereochemistry for the Anionic Oligomerization of Vinyl Pyridines in THF at -78°C

M^+	Anion	Monomer	% Selection	Formal Addition Stereochemistry
Li	$2EP^-$	2VP	91% ± 3	Trans
	$Dimer^-$	2VP	67% ± 5	Trans
	$Trimer^-$	2VP	90% ± 8	Trans
K	$2EP^-$	2VP	75% ± 3	Trans
Li	$2EP^-$	4VP	51% ± 3	Trans

Effect of Degree of Oligomerization

The trimer [9] and the tetramer [10] of oligomerization of monomer [4] with Li as counterion were prepared according to Equations 8 and 9 and purified by column chromatography

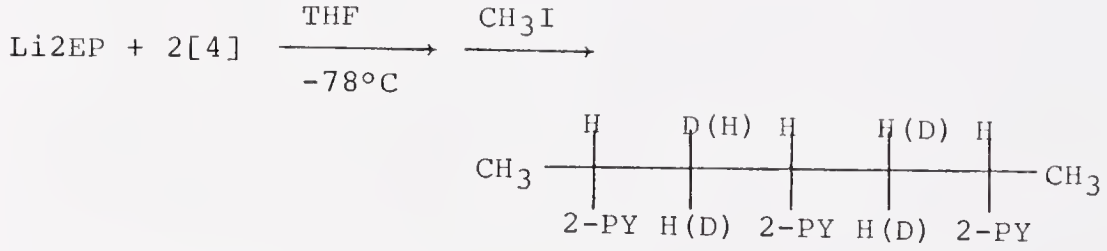

[9]

Equation 8

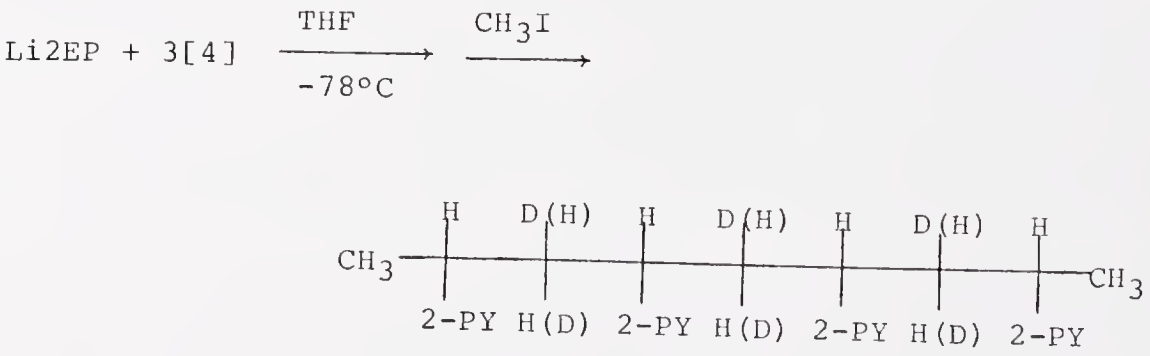

[10]

Equation 9

over alumina. The methylene portions of the 270 MHz ^1H NMR spectra are shown in Figures 16 and 17.

In the trimer spectrum, the relative positions of the erythro and threo positions are the same as in the dimer as ascertained from the relative areas, keeping in mind that the first placement is 91% selective. Calculations correcting for the monomer composition and subtracting the dimer contribution shows a somewhat surprising result in that the interior erythro and threo positions are reversed relative to the outer positions. This was discovered from a comparison with the spectrum of

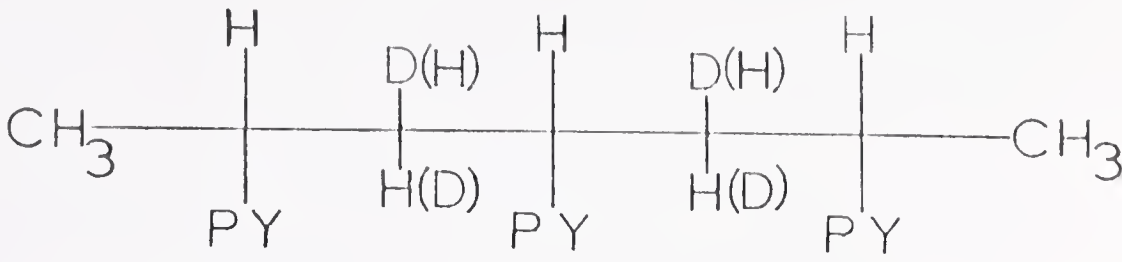

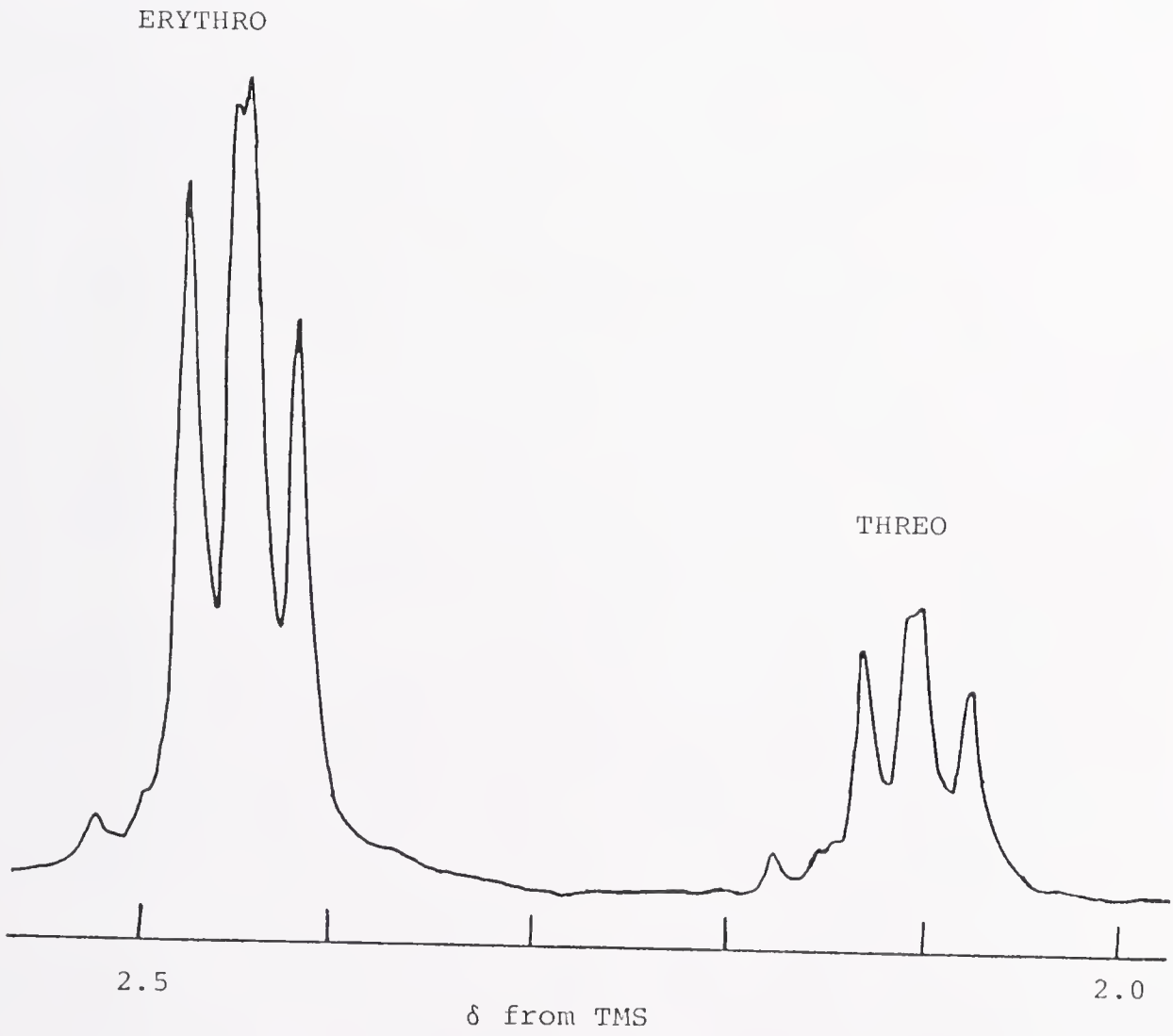

Figure 16. 270 MHz ^{1}H NMR Sprectrum of [9]

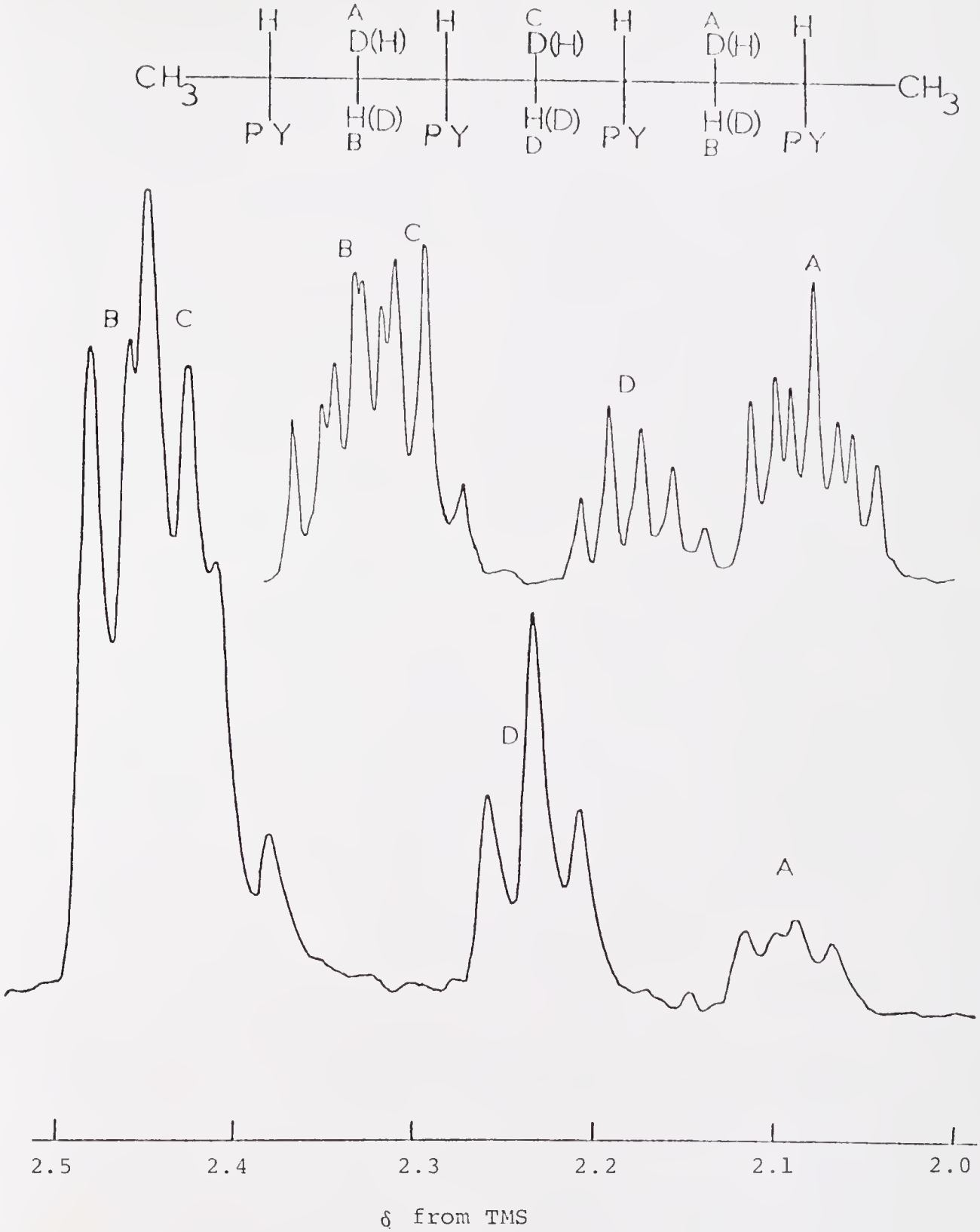

Figure 17. 270 MHz ^{1}H NMR Spectrum of [10]
(Insert: Methylene Spectrum of Protio Compound)

the protonated tetramer, where the absorptions at δ1.98 and δ2.11 are assigned to the interior methylene protons. The sum of the absorptions of the interior protons must equal a third of the total methylene absorption. From this fact, the upfield absorption represents a majority of the interior methylene absorption. As a check, calculations using these assignments lead to the same value for the selectivity of the second addition as obtained from the trimer spectrum. Subtracting the trimer and dimer contributions and correcting for monomer composition yielded a value of about 90% selectivity for the third placement. This is a surprising result, in that the second addition appears to be less selective than either the first or third additions.

Effects of Monomer Structure

In order to study the importance of nitrogen in the 2 position of the ring of the monomer, the cross product [11] was prepared according to Equation 10. As in the oligomeri-

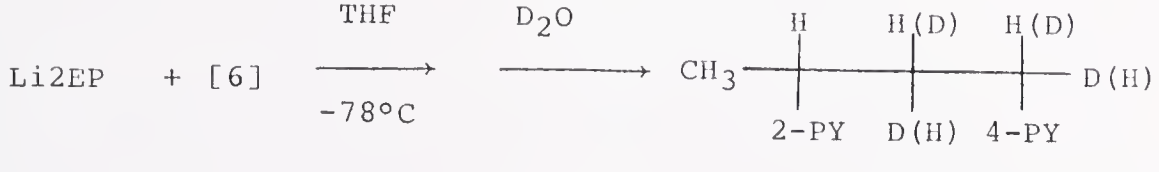

[11]

Equation 10

zation with K as counterion, D_2O was used instead of alkylating with CH_3I to avoid the creation of a second chiral center. The 270 MHz ^1H NMR spectrum of the product is shown in Figure 18. It is apparent that both beta methylene positions are

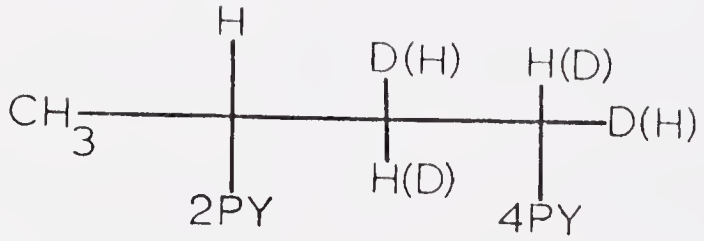

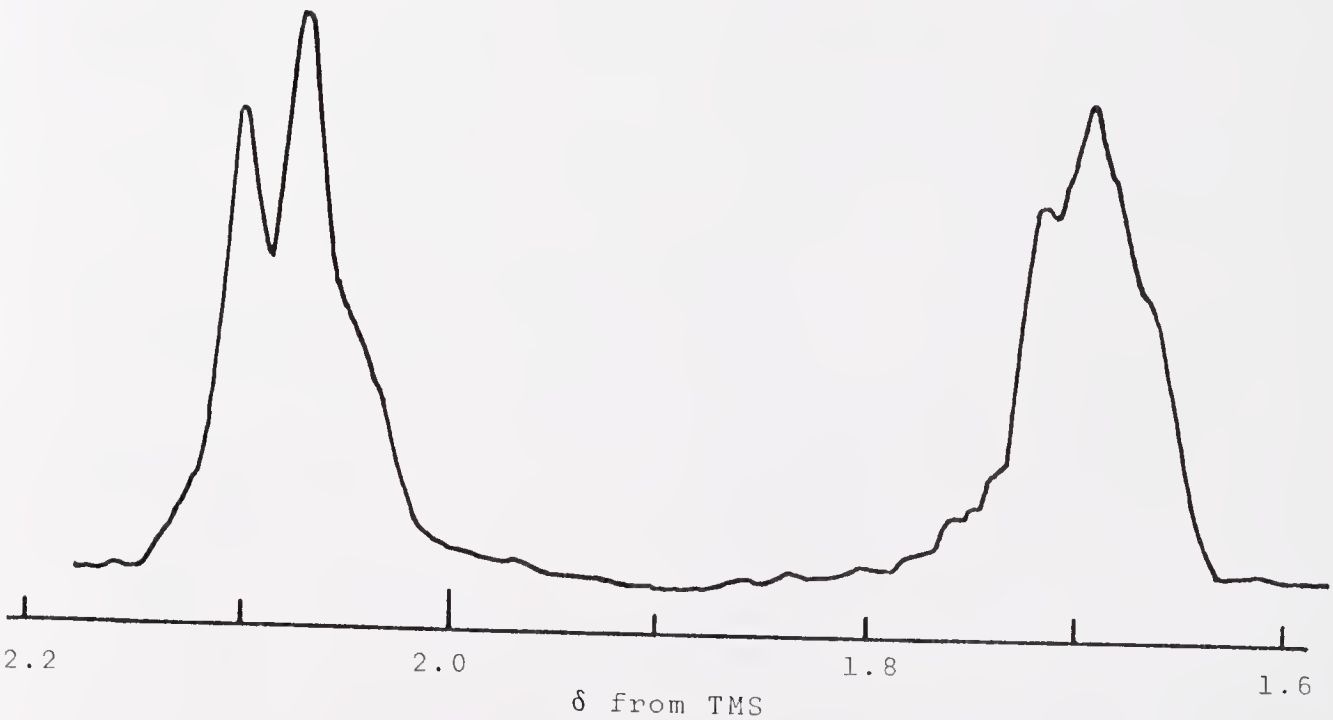

Figure 18. 270 MHz ^{1}H NMR Spectrum of [1]

about equally deuterated, and in fact, integration has shown them to be the same within experimental error.

Discussion

As mentioned in Chapter I, an understanding of beta-carbon stereochemistry is required for a complete understanding of the polymerization mechanism for two reasons. First, the observation of beta-carbon stereoselectivity indicates that the approach of the monomer is controlled, not only with respect to the side of the chain end being approached, but also with respect to the face of the monomer which approaches the chain end. Secondly, if both the placement of deuterium in the monomer and in the polymer is known, then the face of the monomer which approaches the chain end and the mode of opening of the double bond are determined.

Correlation between Anion Geometry and Beta-Carbon Stereochemistry

The beta-carbon stereoselectivities for the first monomer addition to both the Li (91%) and K (77%) salts of 2-ethylpyridine show a strong correlation with the populations of the E isomers (95% for Li and 80% for K). This observation suggests that the monomer addition is being directed in the same manner for both forms of both salts, and that the resulting beta-carbon stereoselectivity is determined by the anion geometry. This is a factor not previously observed or discussed in beta-carbon stereochemistry investigations.

Regarding the nature of the beta-carbon stereoselective process, it is significant that 4-VP adds in a nonselective manner. This is the expected result if coordination of the

incoming monomer with counterion is responsible for guiding monomer approach. Such a coordination of monomer was earlier suggested for 2-VP on the basis of kinetic data (11). The ion pair polymerization rate constant of styrene is accelerated by better cation-solvating media because of an increase in the proportion of loose ion pairs (1). In contrast, the polymerization of 2-VP proceeds more rapidly in poorer solvents (1). This observation was explained by suggesting that the nature of the ion pair structure is the same in all solvents studied, and that coordination of monomer to the cation occurs. In the better solvents the solvent molecules are more tightly bound to the cation and therefore less easily displaced than in poorer solvents.

Model for Addition

It is possible to combine a knowledge of the ion pair structure of alkali salts of 2-EP with the requirement of coordination of monomer in the addition to formulate a model for the propagation step in the polymerization of 2-VP. The approach of incoming monomer can be represented as shown in Figure 19. The cation is in the position above the nodal plane between N and C as discussed earlier. The approach depicted appears preferred from an examination of models and predicts the placement of deuterium in agreement with the assignments made in the meso-di-(2-pyridyl)pentane spectra. The agreement of the beta-carbon stereochemistry with the proportions of the E and Z isomers and the requirement of nitrogen at the number two ring position relative to the vinyl group provides support for this model. The lack of

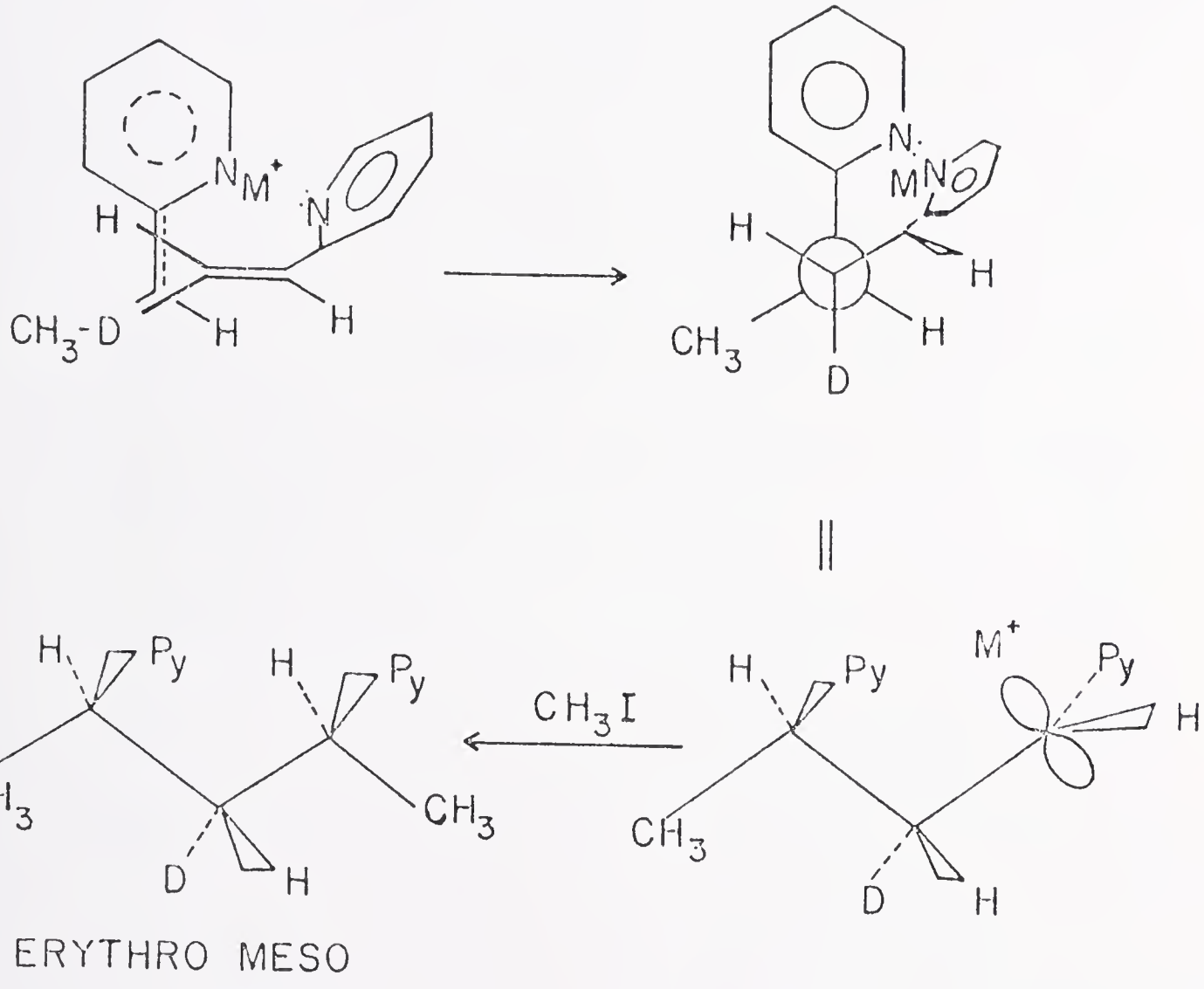

Figure 19. Model for the Addition of 2-Vinylpyridine to M^+2EP^-

agreement for the THF/tetraglyme oligomerization with the proportion of the E isomer in similar conditions is not predicted by the model. However, keeping in mind that the ion pair rate constant of 2-VP polymerization is retarded by cation solvation (11), the addition could well be occurring primarily through a relatively small proportion of uncomplexed salt.

The decrease in selectivity for the second addition and return to greater selectivity in the third addition could be due to a change in rotamer populations and/or the introduction of additional unknown factors. An explanation consistent with the earlier discussion regarding rotamer populations and with the NMR spectra of Li and Na salts of 1,3-di-(2-pyridyl)butane considers the effect of solvation by the penultimate pyridine. An increase in cation solvation in general reduces the proportion of the E isomer (see Table 5), and could thereby reduce the selectivity. The increased selectivity of the third addition could be explained by a steric effect of the antepenultimate ring reducing the effectiveness of the penultimate solvation and returning the rotamer populations to values nearer those of the $2EP^-$ salts. Alternatively, other unknown factors may be entering into the process.

The existence of two different anion geometries at the chain end allows for some interesting speculations. With an equilibrium between E and Z geometries and assuming that the beta-carbon stereochemistry is determined in the manner suggested by this work, the observed beta-carbon stereo-

chemistry will depend not only upon the equilibrium, but also upon the relative rate constants for propagation for the two forms. Since the two ion pair geometries are diastereomeric, in principle, the rates of propagation should be different. Thus, with the E isomer giving erythro product, the erythro/threo ratio should depend upon $k_E\tau_E/k_Z\tau_Z$, where k's and τ's represent rate constants for propagation and lifetimes, respectively. The correlation made between the E/Z ratio and the erythro/threo ratios suggests that $k_E \simeq k_Z$.

The restricted rotation about the C2-Cα bond presents another interesting possibility. The relative rates of formation of the E and Z geometries may differ from the equilibrium values. The experiments in this study were all conducted under conditions of low monomer concentration and hence low rates of propagation. Under conditions of faster propagation, the E/Z and erythro/threo ratios could come under kinetic control leading to results different from the findings of this investigation.

With improved separation techniques, it would be of interest to investigate higher oligomers and polymer to see if the stereochemistry found for the tetramer continues. Calculations from the data of Matsuzaki and Sugimoto (56) indicate that in the Et_2Mg-initiated polymerization of 2-vinylpyridine the placement is approximately 85% specific. Interestingly, the placement is the same as in the current investigation if the chemical shifts are reversed for internal methylene positions as found in the internal methylene protons of the tetramer. The agreement between this work and the

findings in the Et_2Mg initiated polymerization suggests that the trimer result is the anomalous one.

Proposed Model for the Anionic Polymerization of 2-Vinylpyridine

The findings of this investigation, coupled with earlier work on the alpha-carbon stereochemistry, provides an extremely detailed look at the anionic propagation of living poly-(2-vinylpyridine), and suggests a mechanism for the propagation.

The configuration at the chain end is determined by the equilibrium between ion pair diastereomers [12] and [13] shown in Figure 20. The cation is in the position above the plane as discussed in Chapter II. The preferred one is [12] which leads to isotactic placement upon attack by monomer from the cation side of the carbanion. As monomer approaches, it coordinates with the cation through the nitrogen lone pair, which directs the monomer addition as shown in Figure 21 to form the new Cα-Cβ bond. To produce isotactic product, as the cation moves to the new chain end it forms diastereomer [12] at the new site. The net reaction corresponds to trans opening of the double bond.

Applications to Other Anionic Polymerizations

These results may be compared with those of other anionic polymerization systems in which beta-carbon stereochemistry has been studied. The most closely related systems and the most interesting are the polyacrylates (14,15,57-60). Here the observed beta-carbon stereochemistry has an intriguing solvent dependence. The explanation by Fowells *et al.* (14) of the situation in toluene with Li as counterion is shown

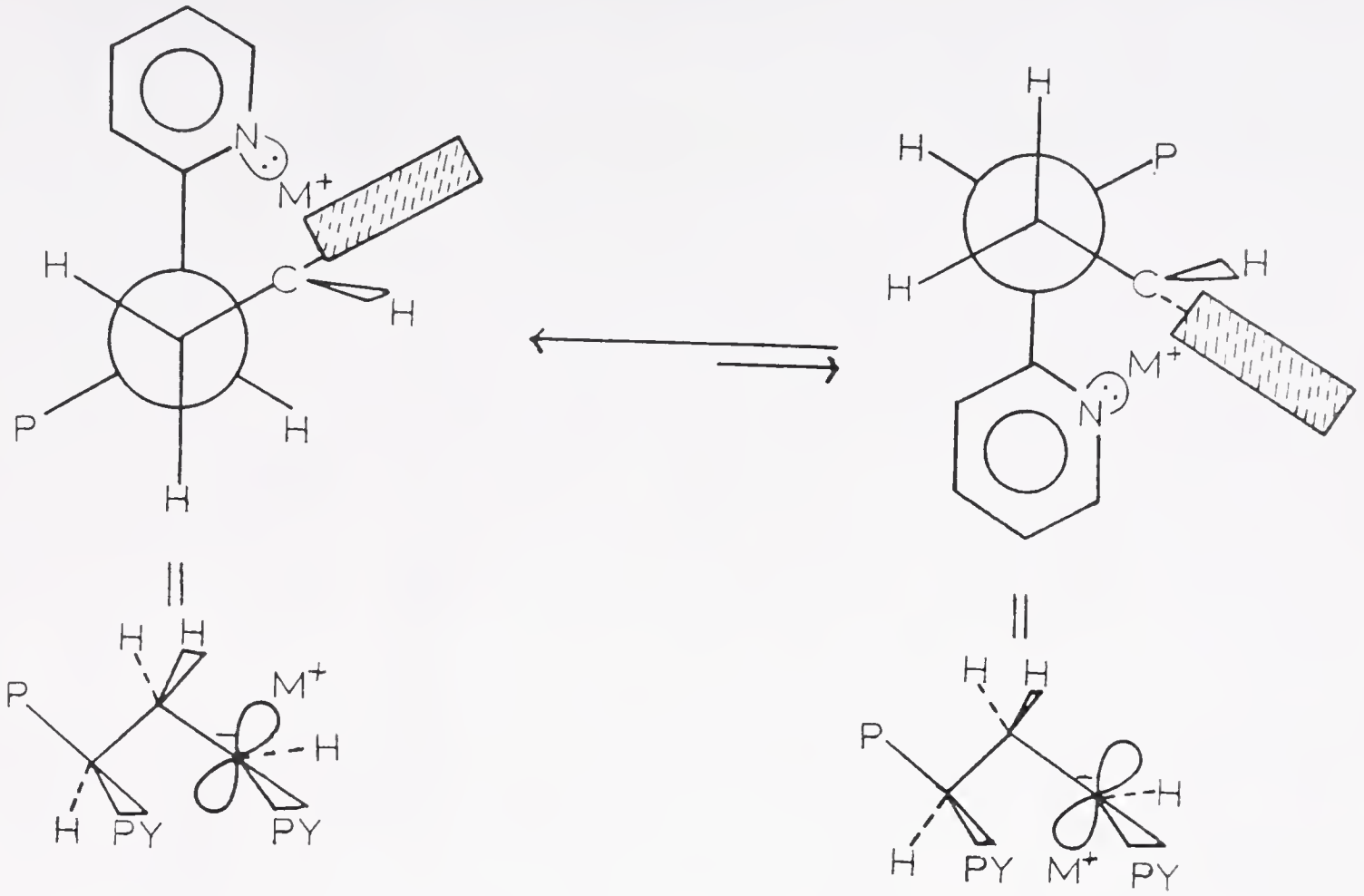

[12] [13]

Figure 20. Configurational Ion Pair Diastereomers in the Anionic Polymerization of 2-Vinylpyridine

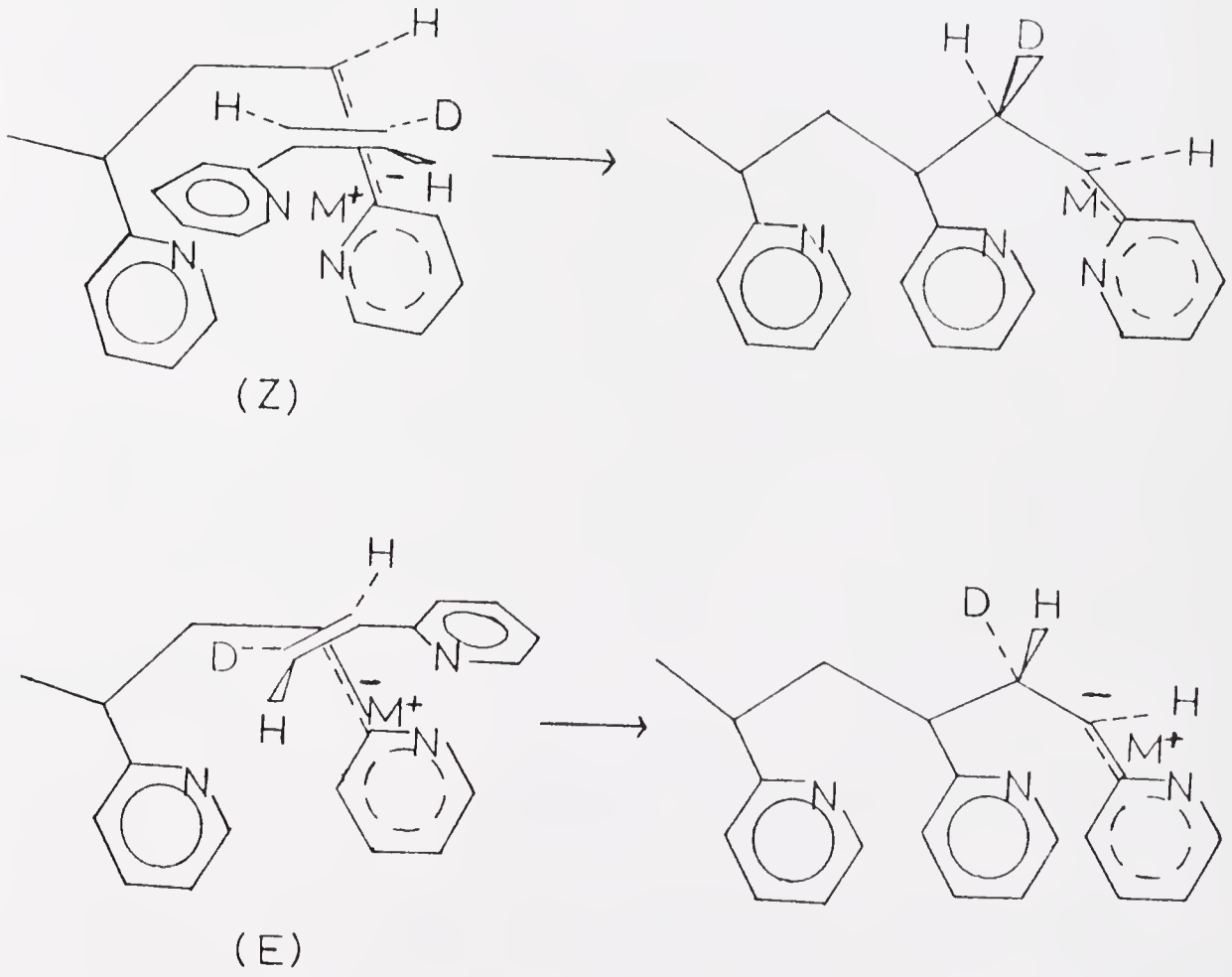

Figure 21. Proposed Mode of Addition in the Anionic Polymerization of 2-Vinylpyridine

in Figure 22. Li is coordinated by the penultimate ester group to produce a preferred configuration at the chain end. The monomer is shown as coordinating with Li in an isotactic approach from the side of the carbanion opposite to the penultimate ester group.

This model illustrates the importance of the cation position. If the cation is in the nodal plane of the anion, the postulated approach is not unreasonable. Fowells et al. (14) did not explicitly consider the effects of anion geometry, but rather assumed that only the Z isomer would exist. The question of cation position is crucial in evaluating the validity of the model. If the cation is in a position above the plane as in the 2EP system, then the proposed direction of approach becomes questionable, since the cation would be separated from the approaching monomer by the chain end. Calculations reported by Eizner and Erussalimsky (32) indicated that the preferred cation position is above the plane of the anion as depicted in Figure 23. If this is correct, then possibilities similar to the 2-VP system exist. Recently, Ireland et al. reported cation and solvent effects on the relative proportions of E and Z carboalkoxy substituted carbanions and the products formed in a study of the ester enolate Claisen rearrangement (61). This work related anion geometry of ester enolates to the stereochemistry of the rearrangement products as illustrated on page 78.

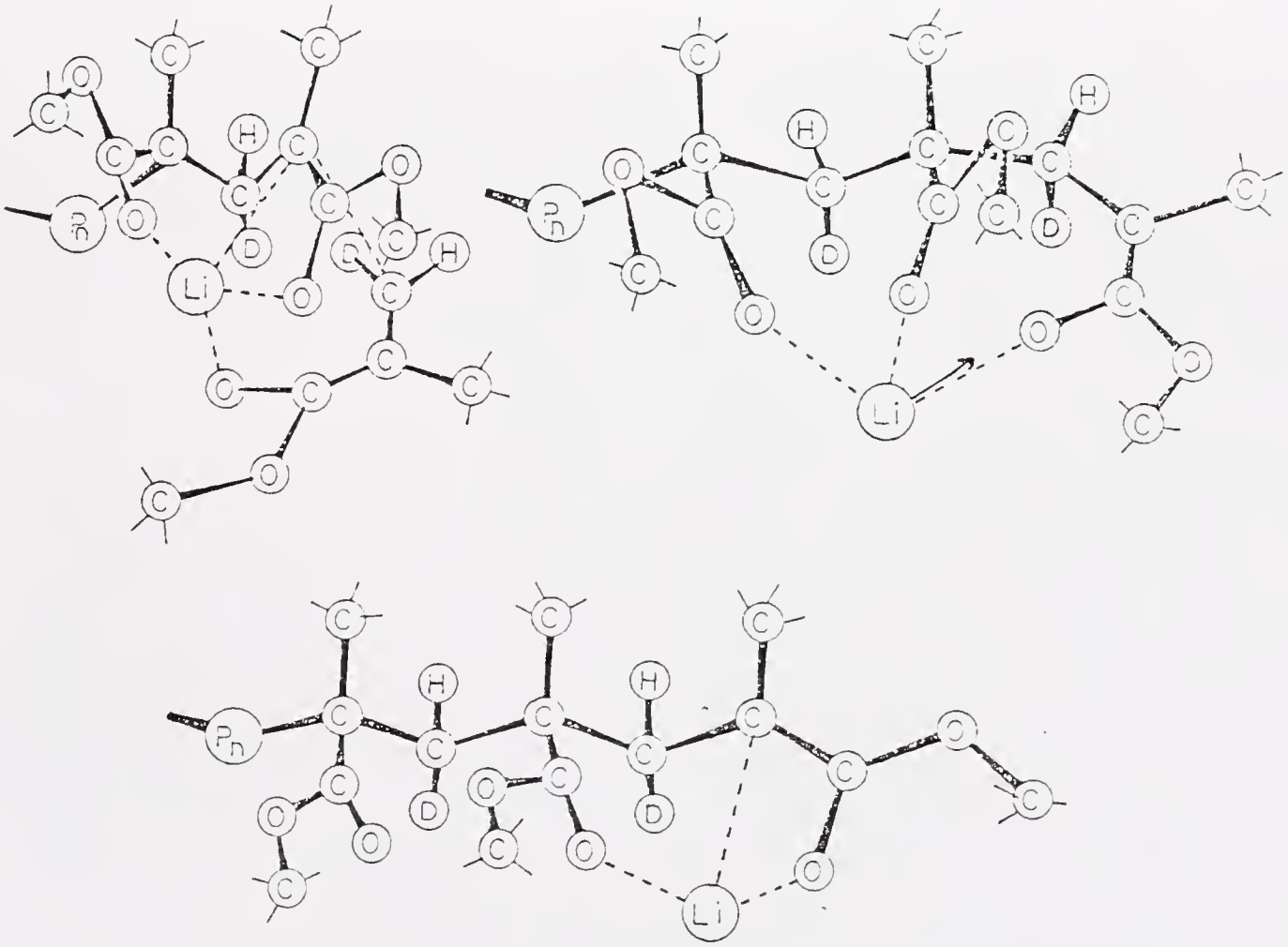

Figure 22. Proposed Mechanism for the Anionic Polymerization of Methy Methacrylate in Toluene

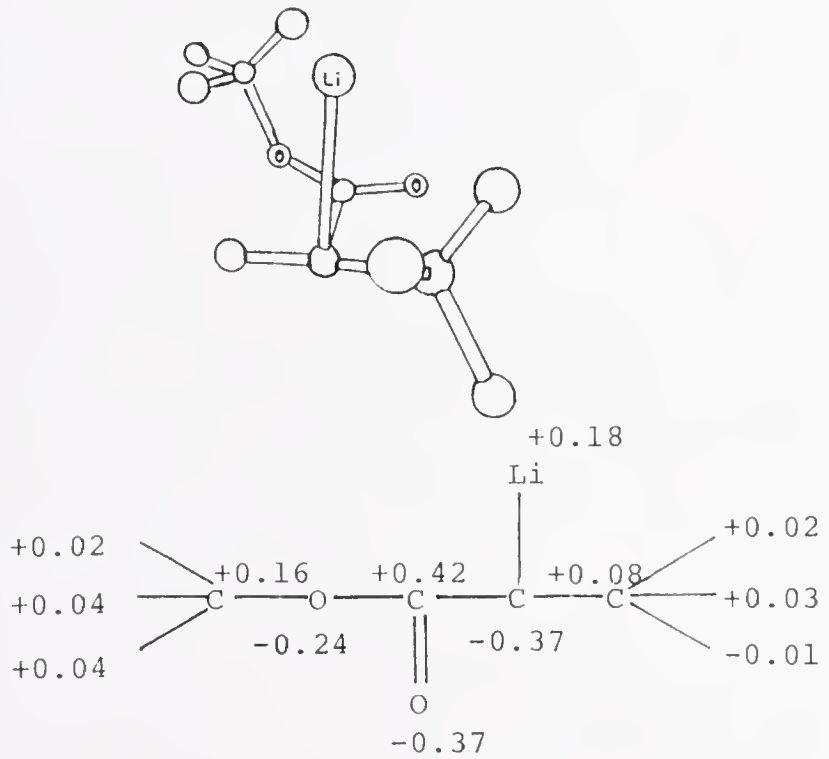

Figure 23. Calculated Ion Pair Structure and Charge Distribution of Li Methyl Propanoate

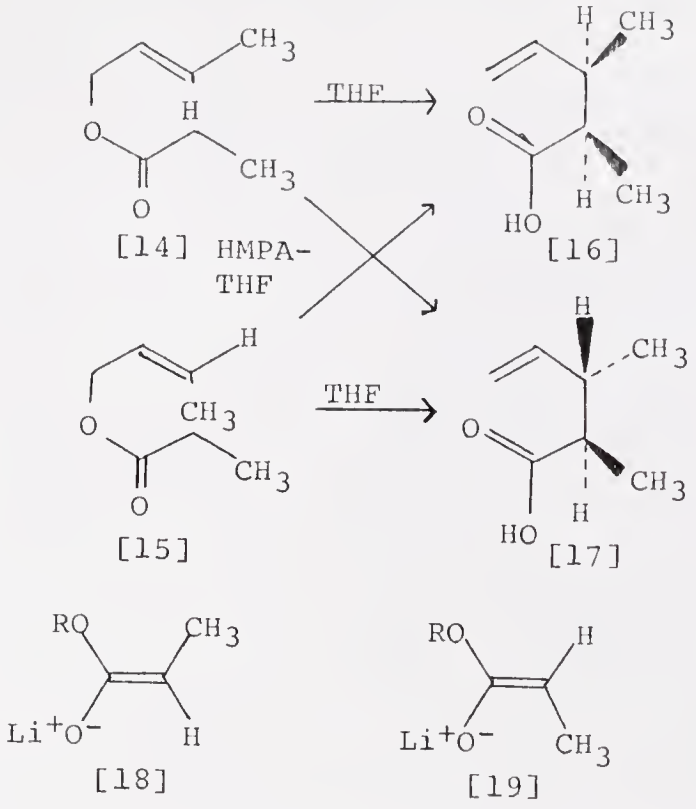

In THF [14] produces [16] and [15] produces [17]. However, after the addition of HMPA, [14] produces [17] and [15] produces [16]. This stereochemical reversal was explained by solvent dependence of stereoselective enolate formation. In THF the Z enolate [18] is formed but in 23% HMPA-THF the E enolate [19] is formed. These findings for an enolate system in which the anion is very similar to the propagating species in the anionic polymerization of acrylates indicate that the anion geometry and beta-carbon stereochemistry in acrylate polymerizations may well show variations with cation and solvent similar to those found in the oligomerizations of vinyl pyridines.

CHAPTER IV

EXPERIMENTAL PROCEDURES

Preparation and Purification of Materials

Solvents

Tetrahydrofuran (THF) was purified by refluxing over sodium-potassium alloy (2 g sodium and 4 g potassium per litter) for about 6 hours, followed by distillation (62). Argon was bubbled through the distillate and fresh metal was added. Approximately 1 g of benzophenone was added prior to degassing on the vacuum line. The formation of the characteristic deep purple color of the benzophenone dianion acted as indicator of the absence of water and oxygen.

Toluene and tetraglyme were stirred over CaH_2 for approximately 12 hours, degassed, and distilled under vacuum.

Solvents and reagents used in monomer synthesis were used as obtained from commercial sources.

2-Ethyl Pyridine

2-Ethyl pyridine was fractionally distilled, stirred over CaH_2, degassed, distilled under vacuum, treated with a carbanion salt available in the laboratory (e.g. poly-α-methylstyrylsodium) to insure purity, and vacuum distilled into glass ampoules equipped with breakseals.

2-Ethylpyridyl Salts

The lithium salt was prepared from n-butyllithium in THF at -78°C. The sodium and potassium salts were prepared from the respective poly-α-methylstyryl salts which were in turn prepared by reaction of α-methylstyrene in THF with an excess of the appropriate metal in the form of a mirror for about 1 hour at room temperature. The salts used for NMR studies were purified by recrystallization from toluene and/or hexane. After replacing the THF with toluene or hexane, the solution was placed in the freezer (-20°C) to induce the formation of crystals. The volume was adjusted by distilling solvent to or from the solution until crystallization occurred within a couple of hours after placing the solution in the freezer. The THF was then removed by leaving the salts on the vacuum line for several hours before adding THF-d_8.

Deuterated 2-Vinylpyridine

The deuterated 2-vinylpyridines were prepared by Cr^{II} reduction of 2-ethynyl pyridine. The 2-ethynylpyridine synthesis was based on the one by Leaver et al. (64). The synthetic route is shown in Figure 24. 2-Vinylpyridine (160 g) in CCl_4 (250 ml) was added dropwise to a mechanically stirred, ice-cooled solution of Br_2 (88 ml) in CCl_4 (350 ml). The solution was decanted from a gummy mass and evaporated under reduced pressure at 40°C to remove solvent and unreacted 2-vinylpyridine. The viscous crude dibromide (282 g) had the expected NMR with the following absorptions

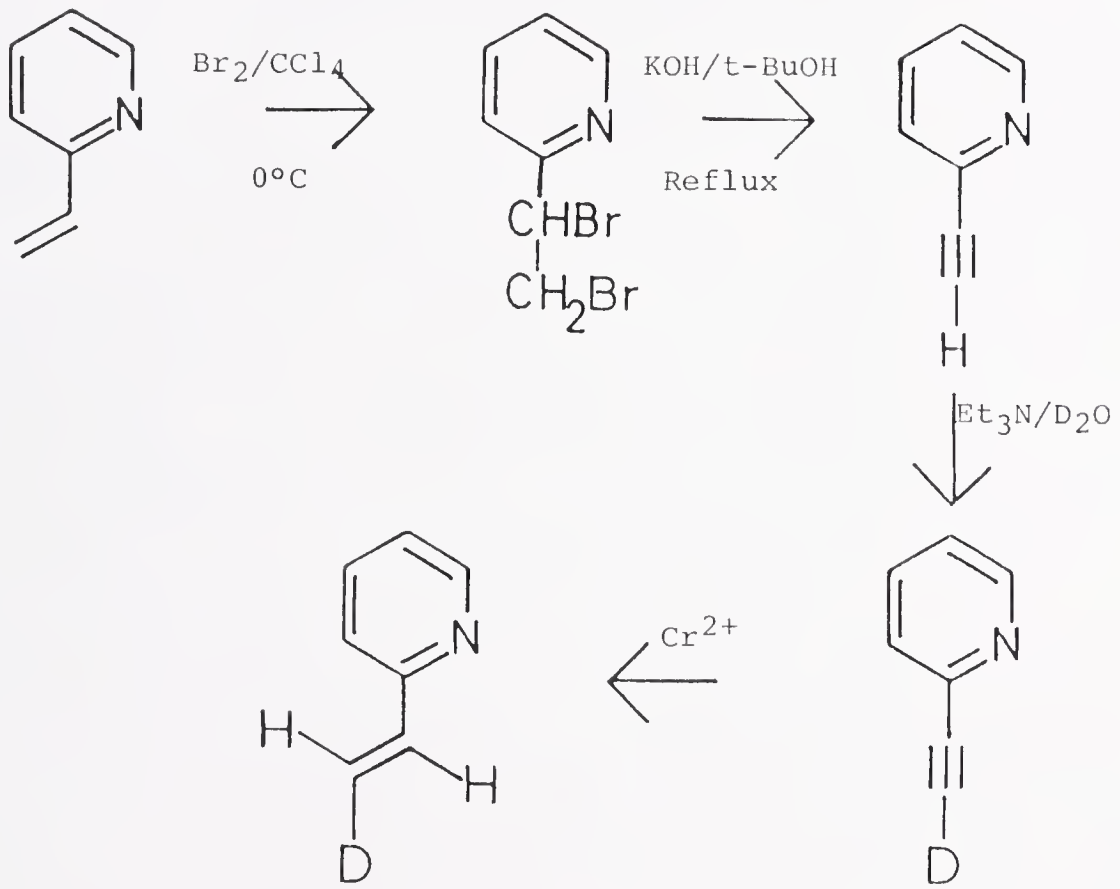

Figure 24. Synthetic Scheme for Deuterated 2-Vinylpyridine

in CCl_4: doublet, δ 8.05 (1H); triplet, δ 7.65 (1H): multiplet, δ 7.2 (2H): quartet, δ 5.25 (1H); quartet, δ 4.0 (1H). The quartets indicate a preferred conformation for the ABX system resulting in differing coupling constants, J_{AB} = 9.3, J_{AX} = 4.9 Hz, J_{BX} = 10.2 Hz.

The crude dibromide (282 g) in t-butanol (200 ml) was added, under N_2 during a 40 minute period, to KOH pellets (250 g) in vigorously stirred, refluxing t-butanol (450 ml) containing hydroquinone (3 g). After the addition was completed, the solution was refluxed and stirred for an additional 1.5 hours, diluted with ether (500 ml) and filtered from an amorphorus black solid. The filtrate was washed with water and the aqueous phase was extracted twice more with ether. The ether solutions were combined, washed with water, dried over $MgSO_4$, and evaporated under reduced pressure to yield a dark brown liquid, which, upon distillation, produced 2-ethynylpyridine (16.2 g, 10.1% yield based upon 2-vinylpyridine), b.p. 74-76°C/12 mm. The ^1H NMR spectrum in CCl_4 was: doublet, δ 8.5 (1H): multiplet, δ 7.4 (3H), singlet, δ 3.35 (1H). Lowering the pressure to 0.25 mm Hg yielded a distillate at 80°C which was a mixture of Z-2(2'-bromoethenyl)pyridine and the E isomer in the proportion 70% Z and 30% E as determined by NMR with assignments based on cis and trans coupling constants.

2-Ethynylpyridine (10 g) and triethylamine (1 g) were vigorously stirred for approximately 0.5 hours (65). The mixture was twice extracted with ether. The ether extracts

were combined, evaporated under reduced pressure, and treated again with D_2O in the same manner. Analysis of the product by NMR showed the exchange to be essentially complete (98% D).

Reduction of the d_1-2-ethynylpyridine was effected by Cr^{II}/H_2O, a reagent used for reducing a variety of acetylenes by Castro and Stephens (66). To prepare a stock solution, hydrated $Cr_2(SO_4)_3$ (343 g) was dissolved in H_2O (2 l) while bubbling N_2 through the system. After adding purified zinc powder (89 g), the mixture was stirred overnight in a flask equipped with a serum cap at room temperature. Filtration was not required, provided that the zinc was allowed to settle before removing solution with a syringe. The clear blue solution had $Cr^{II} \simeq 0.7$ N and pH $\simeq$ 3.5. The stock solution was standardized by removing 2 ml aliquots and injecting into an aqueous solution containing excess $FeCl_3$ under nitrogen. The resulting solution was then titrated with 0.1017 N $Ce(SO_4)_2$ to a green phenanthroline end point. The reduction of d_1-2-ethynylpyridine was carried out at room temperature under a nitrogen atmosphere. A 10% excess of Cr^{II} solution was transferred to a reaction flask containing the 2-ethynyl-pyridine. The addition of the Cr^{II} solution was accompanied by an immediate color change from the clear blue of Cr^{II} to the dark green of the Cr^{III}. Titration of aliquots confirmed that the reaction was complete almost immediately. The resulting solution was neutralized with $NaHCO_3$ which precipitated chromic

hydroxide. After filtration the solution was extracted three times with ether. The combined ether extracts were dried over $MgSO_4$ and evaporated under reduced pressure. After stirring for about 4 hours over CaH_2 the liquid yielded upon vacuum distillation E-β-d_1-2-vinylpyridine. The NMR spectrum (Figure 25) indicated the E product to represent 91% of the deuterated material.

The Z-α,β-d_2-2-vinylpyridine was prepared similarly, except that 2-ethynylpyridine was reduced by Cr^{II} in D_2O.

Preparation of Deuterated 4-Vinylpyridine

E-β-d_1-4-vinylpyridine was prepared by Cr^{II} reduction of d_1-4-ethynylpyridine. Synthesis of 4-ethynylpyridine was achieved based on the procedure reported by Gray et al. (67) as shown in Figure 26. 4-Vinylpyridine hydrochloride (m.p. 240-243°C) was prepared by bubbling HCl through a toluene solution of 4-vinylpyridine at -78°C. The HCl was conveniently prepared by dripping concentrated H_2SO_4 onto NaCl in a flask warmed by a hotplate. The salt was collected by filtration and washed with hexane. 4-Vinylpyridine hydrochloride (68 g) in 350 ml of $CHCl_3$, cooled in an ice bath and vigorously stirred, was treated by dropwise addition of Br_2 (150 g). After the addition was completed, the reaction mixture was stirred for 1 hour at ice-bath temperature and 1 hour at room temperature. The mixture was diluted with ether and the precipitated orange oil was then treated with 300 ml of acetone to yield the white, crystalline hydrochloride salt of 4-vinylpyridine dibromide (122 g, m.p. 148-150°C).

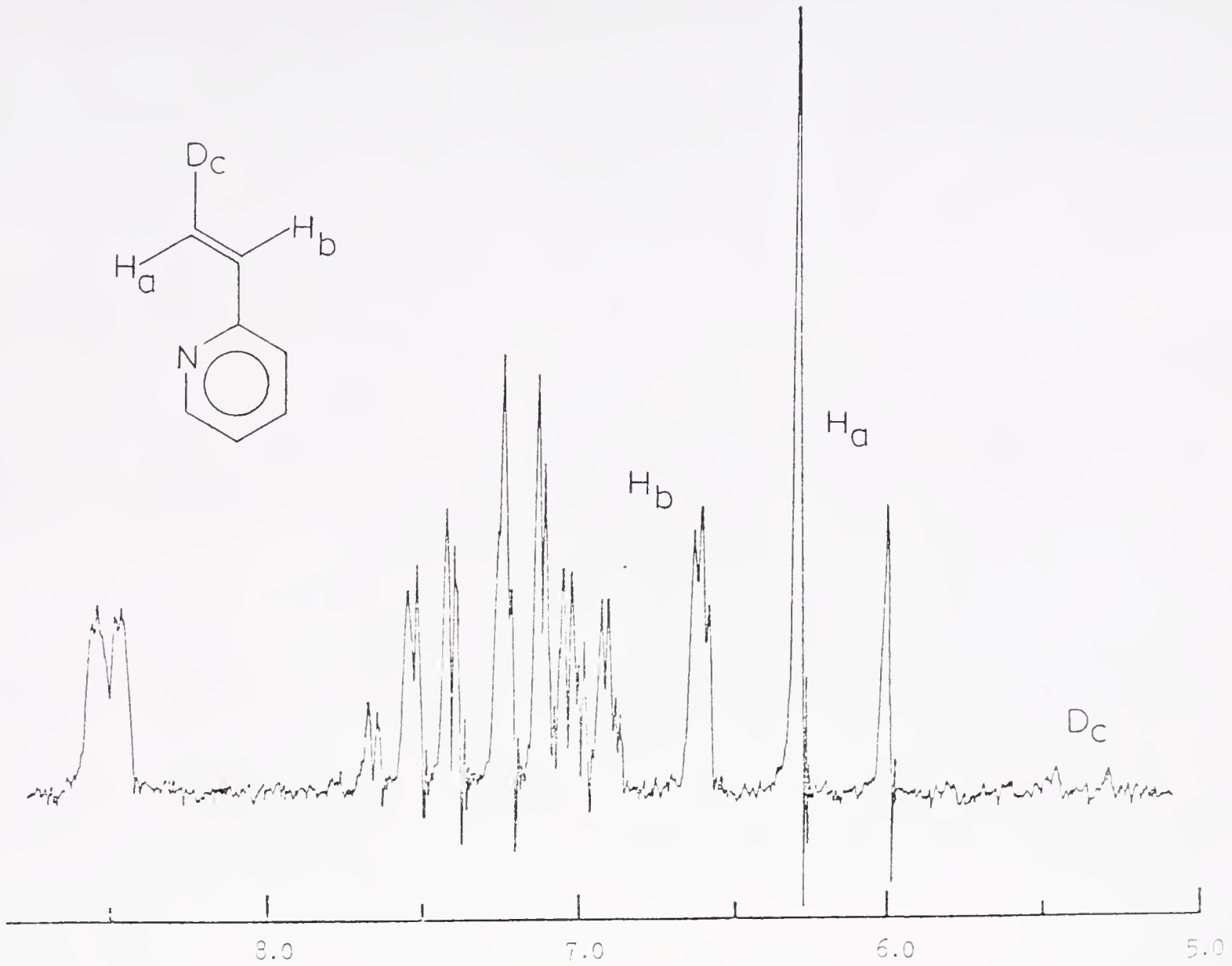

Figure 25. 60 MHz ^{1}H NMR Spectrum of E-β-d_1-2-Vinylpyridine

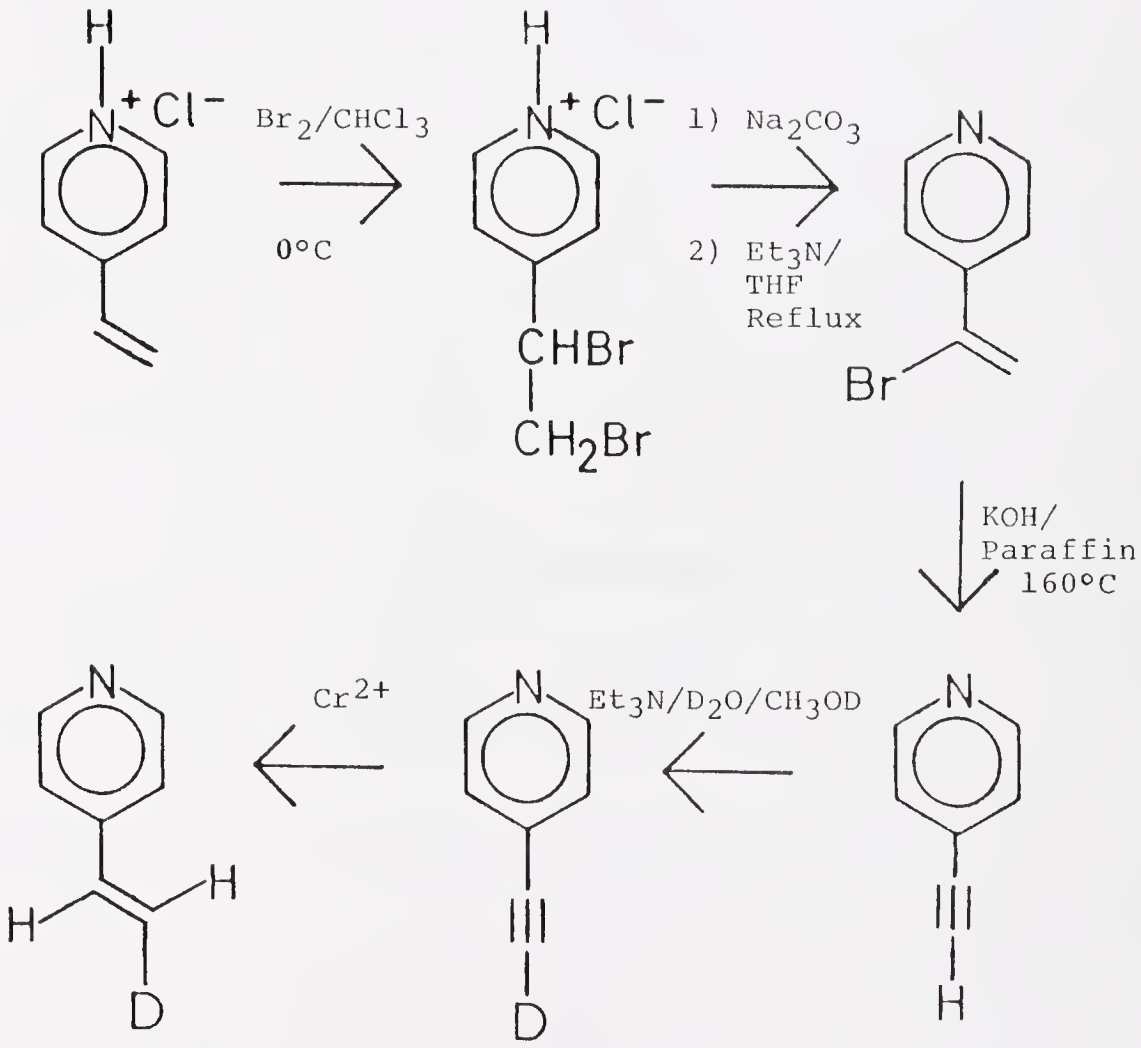

Figure 26. Synthetic Scheme for Deuterated 4-Vinylpyridine

The salt (60 g) was treated with 10% Na_2CO_3 and the resulting base was extracted into ether. The ether extracts were dried over $MgSO_4$, concentrated under reduced pressure to 350 ml and treated with triethylamine (22 g) in tetrahydrofuran. The mixture was stirred for 2 hours at room temperature and then refluxed for 3 hours. Triethylamine hydrobromide which had precipitated was filtered off and the filtrate evaporated to produce 35 g of a dark amber oil. The NMR spectrum of the oil in CCl_4 was consistent with the structure of 4-pyridyl-1-bromoethylene: multiplet, δ 8.53 (2H); multiplet, δ 7.37 (2H); doublet, δ 6.29 (1H); doublet, δ 5.85 (1H): $^2J_{AB}$ for the vinyl protons, 2.1 Hz.

The crude 4-pyridyl-1-bromoethylene (35 g) was added in 5 ml portions through a dropping funnel to an intimate mixture of 56 g of powdered KOH and 50 g of paraffin (m.p. 56-58°C), which was magnetically stirred and heated by an oil bath to 160°C under a reduced pressure of about 200 mm. The pressure was held at 200 mm for 2 minutes after each addition, and then slowly reduced to 2 mm as the product distilled out of the reaction mixture. The product was collected in the form of white crystals on the side of the condenser and in the receiving flask which was cooled with a dry-ice/isopropanol bath. The product was recrystallized to yield 3.5 g of 4-ethynylpyridine (m.p. 95-97°C), 18% overall yield from 4-vinylpyridine, NMR spectrum: δ 8.6 (2H): multiplet δ 7.20 (2H); singlet, δ 3.22 (1H).

Exchange of the acetylenic proton was carried out as described for 2-ethynylpyridine.

Reduction was carried out with chromous ion in a manner similar to the reduction of 2-ethynylpyridine. The 4-ethynylpyridine was dissolved in CH_3OD (1 g in 4 ml) prior to the reduction to produce a homogeneous system. Use of CH_3OH resulted in rapid exchange. The reduction showed an interesting temperature dependence. At room temperature NMR analysis of the product showed the Z isomer to predominate by a factor of 60% - 40% in contrast to the stereochemistry of reduction for 2-ethynylpyridine and other acetylenes previously reported (66). An attempt to improve the stereoselection by cooling in an ice bath to 2°C resulted in a 65% to 35% mixture, but under these conditions the E isomer predominated. The NMR spectrum of the latter product is reproduced in Figure 27.

Oligomerizations

Oligomerization of E-β-d_1-2-Vinylpyridine with Li as Counterion (63)

The apparatus used for the reaction is shown in Figure 28. n-Butyllithium (17 ml of 1.6 M in hexane) was injected into the apparatus which had been flushed with argon for 15 minutes. The inlet was capped with a rubber septum and the apparatus was evacuated. The hexane was removed by distillation prior to condensing tetrahydrofuran (200 cc) in the reaction flask. 2-Ethylpyridine (2.5 ml) was distilled into the flask which was cooled to -78°C in a dry ice-

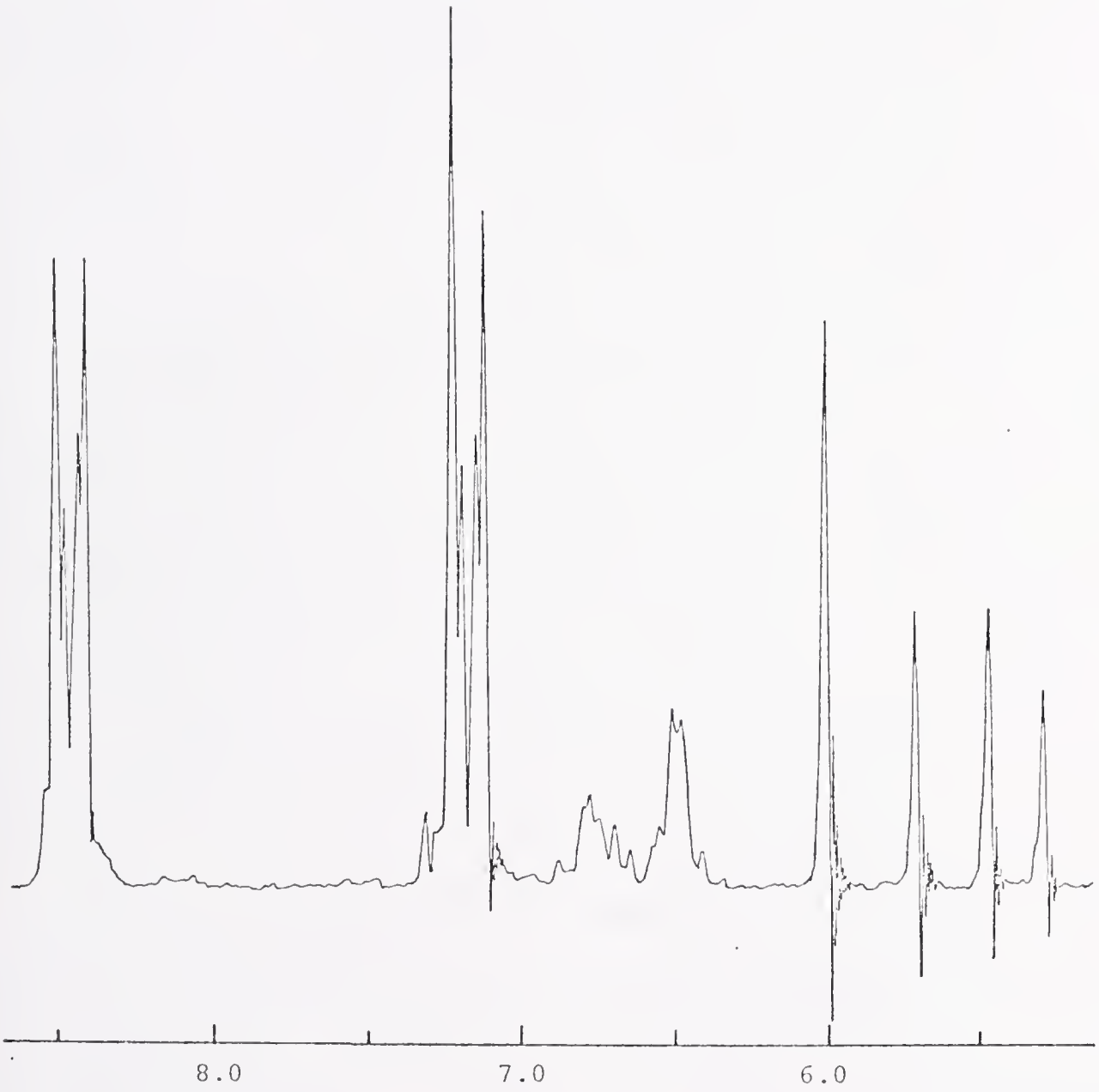

Figure 27: 60 MHz ^{1}H NMR Spectrum of E-β-d_1-4-Vinylpyridine

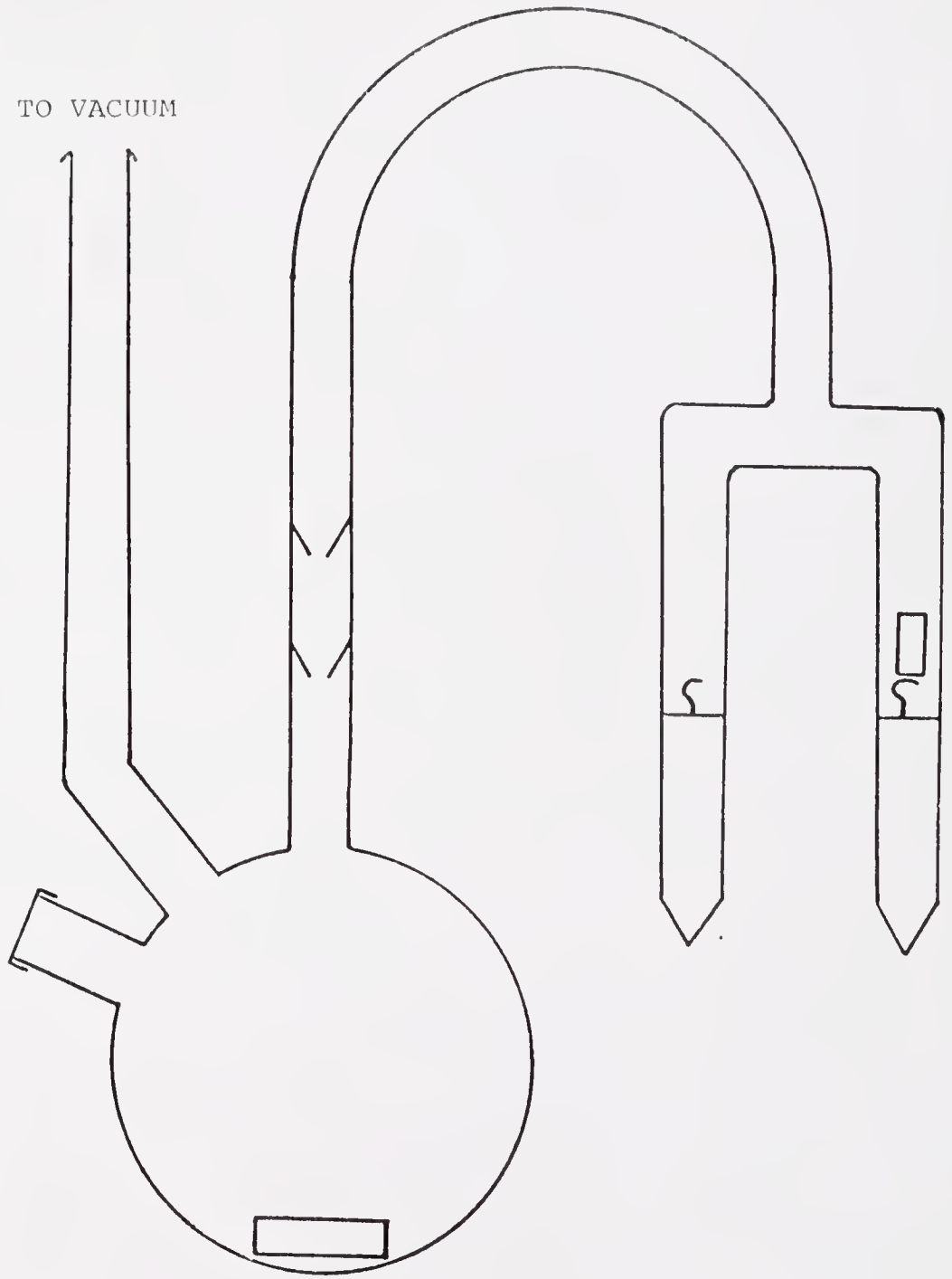

Figure 28. Apparatus for Anionic Oligomerization of Vinyl Pyridines

isopropanol bath. The solution was allowed to warm up slowly to room temperature to allow removal of the butane by distillation. After cooling the system again to -78°C, the ampoule containing the deuterated monomer was opened. The monomer was distilled into the system during a period of 1 to 2 hours. The distillation was slowed by cooling the monomer ampoule with ice water to reduce the formation of polymer. The reaction was terminated with CH_3I which had been dried over CaH_2 and degassed. The solvent was removed under reduced pressure and the mixture of oligomers dissolved in 10% HCl. The solution was washed with ether and neutralized with Na_2CO_3. The resulting base was extracted into ether. After drying over $MgSO_4$ and removing the ether under reduced pressure, the 2,4-di-(2-pyridyl) pentane was conveniently obtained by distillation (110-114°C, 0.25 mm).

Isolation of Trimer and Tetramer (19)

Isolation of the trimer and tetramer was achieved using column chromatography. Neutral alumina of Brockman Activity I (80 - 200 mesh) which had been stored in a 110°C oven overnight was used. The elution began with a 50/50 (vol/vol) mixture of ether and ligroin. The composition was varied until pure ether was the eluting solvent. A 50/50 mixture of ether and ethyl acetate was then used. Fractions containing relatively pure trimer and tetramer were obtained. The trimer and tetramer required use of 270 MHz NMR to resolve the methylene protons.

Oligomerization of E-β-d_1-Vinylpyridine with Li as Counterion; Tetraglyme Added (19)

The reaction was carried out in a similar manner to that described above. The tetraglyme was added to the 2-ethylpyridyl salt at -78°C prior to monomer addition.

Oligomerization of Z-α,β-d_2-2-Vinylpyridine with K as Counterion (19)

The reaction was carried out similarly to that using Li as counterion. The 2-ethylpyridyl carbanion was generated by distilling 2-ethyl-pyridine onto a tetrahydrofuran solution of potassium α-methylstyrene oligomer. The reaction was stopped by distilling D_2O into the reaction vessel. The 1,3-di-(2-pyridyl)butane product was analyzed by 270 MHz NMR.

Cross Experiment: Lithium 2-Ethylpyridine with E-β-d_1-4-Vinylpyridine (19)

The procedure used was the same as that for the anionic oligomerization of 2-vinylpyridine with Li as counterion. The reaction of n-BuLi with 2EP in THF at -78°C generated Li2EP. Slow distillation of E-β-d_1-4-vinylpyridine onto the solution at -78°C followed by the addition of D_2O completed the preparation. Following the usual workup, the product was vacuum distilled (105-110°C, 0.25 mm) and analyzed by 270 MHz NMR.

Selectivity of Placement

The selectivity of placement was determined from the ^1H NMR spectra as follows:

1. The upfield and downfiled areas corresponding to the beta-carbon absorptions were determined and normalized to a total area of 1.

2. The total area actually represents 1 + f_H protons where f_H is the fraction of undeuterated monomer, since each undeuterated monomer contributes to both regions. Each absorption was therefore corrected for undeuterated monomer by subtracting $f_H/1 + f_H$.
3. Corrected areas were again normalized to a total area of 1.
4. Correction for proportion of E to Z deuterated monomer was made according to the equation

$$f_E X + (1 - f_E)\ (1 - X) = A_L$$

where f_E id the fraction of E deuterated monomer, X is the fraction of preferred placement, and A_L is the corrected and normalized area for the largest absorption from step 3.

UV-Conductance

For the UV-conductance studies the appropriate sample was introduced by means of a breakseal into an evacuated glass vessel possessing 0.2 cm, 1 cm, 5 cm, and 10 cm UV cells and a conductance cell. The concentration of carbanion was determined before and after conductance measurements using a Beckman Acta V UV/VIS spectrophotometer. Conductance measurements were made in a cell, designed for solutions of very low conductance, of cell constant 0.083 as determined from the conductance of KCl solutions. A General Radio 1673-A

Automatic Capacitance Bridge operating at 1 kHz was connected to a General Radio 1672-A Digital Control Unit also operating at 1 kHz. Additions of dibenzo-18-crown-6 and [2.2.2] cryptand were performed by opening a breakseal under high vacuum.

CNDO/2 Calculations

The CNDO/2 program used for the calculations is a modified version of the program described by Pople and Beveridge (34) which is available from the Quantum Theory Project at the University of Florida. Details concerning the modifications are available from the Quantum Theory Project.

REFERENCES

1. M. Szwarc, in "Ions and Ion Pairs in Organic Reactions," Vol. 2, M. Szwarc, Ed., Wiley Interscience, New York, N.Y., 1974, Chap. 4.

2. T.E. Hogen-Esch, in "Advances in Physical Organic Chemistry," V. Gold and D. Bethell, Eds., Academic Press, New York, 1977.

3. M. Szwarc, in "Carbanions, Living Polymers, and Electron-Transfer Processes," Wiley, New York, N.Y., 1968, Chap. 7, 8.

4. H. Hirohara and N. Ise, J. Polym. Sci., Part D, 6, 295 (1972).

5. T. Shimomura, K.J. Tolle, J. Smid, and M. Szwarc, J. Am. Chem. Soc., 89, 976 (1967).

6. T. Shimomura, J. Smid, and M. Szwarc, J. Am. Chem. Soc., 89, 5743 (1967).

7. G.V. Schulz, L.L. Bohrn, M. Chmelin, G. Lohr, and B.J. Schmitt, IUPAC Advances Pol. Sci., 9, 1 (1972).

8. D.N. Bhattacharyya, J. Smid, and M. Szwarc, J. Phys. Chem., 69, 624 (1965).

9. F.S. Dainton, G.C. East, G.A. Harpell, N.R. Hurworth, K.J. Ivin, R.T. Laflair, R.H. Pallen, and K.M. Hui, Makromol. Chem., 89, 257 (1965).

10. F.S. Dainton, K.M. Hui, and K.J. Ivin, Europ. Polymer J., 5, 382 (1969).

11. M. Fisher and M. Szwarc, Macromolecules, 3, 23 (1970).

12. M. Shinohara, J. Smid, and M. Szwarc, Chem. Comm. (London), 1232 (1969).

13. F.A. Bovey, in "Polymer Conformation and Configuration," Academic Press, New York, N.Y., 1969.

14. W. Fowells, C. Schuerch, F.A. Bovey, and F.P. Hood, J. Am. Chem. Soc., 89, 1396 (1967).

15. C. Schuerch, W. Fowells, A. Yamada, F.A. Bovey, F.P. Hood, and E.W. Anderson, J. Am. Chem. Soc., 86, 4481 (1964).

16. C.F. Tien and T.E. Hogen-Esch, J. Am. Chem. Soc., 98, 7109 (1976).

17. a) A.I. Meyers, G. Draus, K. Kamata, and M. Ford, J. Am. Chem. Soc., 98, 567 (1976); b) E.L. Eliel, A. Abatjoglou, and A.A. Hartman, J. Am. Chem. Soc., 94, 4786 (1972); c) H.M. Walborsky and A.E. Young, J. Am. Chem. Soc., 86, 3288 (1964); d) T. Durst and M. Molin, Tetrahedron Lett., 63 (1975).

18. D.J. Cram, in "Fundamentals of Carbanion Chemistry," Academic Press, New York, N.Y., 1965.

19. C.F. Tien and T.E. Hogen-Esch, J. Polym. Sci., B, Polymer Lett., May, 1978.

20. C.F. Tien and T.E. Hogen-Esch, Unpublished results.

21. M. Tardi and P. Sigwalt, Europ. Polymer J., 8, 151 (1972).

22. M. Tardi and P. Sigwalt, Europ. Polymer J., 9, 1369 (1973).

23. C.B. Wooster, J. Am. Chem. Soc., 59, 377 (1937).

24. K. Takahashi, K. Konishi, M. Ushio, M. Takaki, and R. Asami, J. Organomet. Chem., 50, 1 (1973).

25. A. Allerhand and H.S. Gutowsky, J. Chem. Phys., 41, 2115 (1964).

26. G.W. Castellan, in "Physical Chemistry, Addison-Wesley, Reading, Mass., 1971, pp. 740-745.

27. G.E. Maciel, J.W. McIver, Jr., N.S. Ostlund, and J.A. Pople, J. Am. Chem. Soc., 92, 1 (1970).

28. J.B. Stothers, in "Carbon-13 NMR Spectroscopy," Academic Press, New York, N.Y., 1972.

29. G.C. Levy and G.L. Nelson, in "Carbon-13 Nuclear Magnetic Resonance for Organic Chemists," Wiley-Interscience, New York, N.Y., 1972.

30. A. Bongini, C. Cainelli, G. Cardillo, P. Palmieri, and A. Umani-Rochi, J. Organomet. Chem., 110, 1 (1976).

31. R.J. Bushby and A.S. Patterson, J. Organomet. Chem., 132, 163 (1977).

32. Y.Y. Eizner and B.L. Erussalimsky, Europ. Polymer J., 12, 59 (1976).

33. J.F. Sebastian, B. Hsu, and J.R. Grunwell, J. Organomet. Chem., 105, 1 (1976).

34. J.A. Pople and D.L. Beveridge, in "Approximate Molecular Orbital Theory," McGraw-Hill, New York, N.Y., 1970.

35. "Talbes of Interatomic Distances and Configurations in Molecules and Ions," The Chemical Society, London, 1965.

36. J.A. Zoltewicz and L.S. Helmick, J. Org. Chem., 38, 658 (1973).

37. A.J. Gordon and R.A. Ford, in "The Chemist's Companion," John Wiley and Sons, Inc., New York, N.Y., 1972.

38. J.A. Pople and G.A. Segal, J. Chem. Phys., 44, 3289 (1966).

39. C.J. Chang, R.F. Kiesel, and T.E. Hogen-Esch, J. Am. Chem. Soc., 97, 2805 (1975).

40. M. Tardi, D. Rouge, and P. Sigwalt, Europ. Polymer J., 3, 85 (1967).

41. M. Szwarc, in "Ions and Ion Pairs in Organic Reactions," Vol. 1, M. Szwarc, Ed., Wiley Interscience, New York, N.Y., 1972.

42. L.M. Jackman and S. Sternhill, in "Applications of Nuclear Magnetic Resonance Spectroscopy in Organic Chemistry," Pergamon Press, New York, N.Y., 1969, pp. 291-292.

43. H. Spieseche and W.G. Schneider, Tetrahedron Lett., 468 (1961).

44. T. Tokuhiro and G. Fraenkel, J. Am. Chem. Soc., 91, 5005 (1969).

45. J. Bloor and D.L. Breen, J. Am. Chem. Soc., 89, 6835 (1967).

46. F.J. Kronzer and V.R. Sandel, J. Am. Chem. Soc., 94, 5750 (1972).

47. J.A. Dixon, P.A. Gwinner, and D.C. Lini, J. Am. Chem. Soc., 87, 1379 (1965).

48. K.H. Wong, G. Konizer, and J. Smid, J. Am. Chem. Soc., 92, 666 (1970).

49. S.P. Patterman, I.L. Karle, and G.D. Stucky, J. Am. Chem. Soc., 92, 1150 (1970).

50. R. Waach, L.D. McKeever, and M.A. Doran, Chem. Commun., 117 (1969).

51. M. Schlosser and J. Hartmann, J. Am. Chem. Soc., 98, 4674 (1976).

52. V.R. Sandel, S.V. McKinley, and H.H. Freedman, J. Am. Chem. Soc., 90, 495 (1967).

53. R.B. Bates, D.W. Grosselink, and J.A. Kaczynski, Tetrahedron Lett., 205 (1967).

54. D. Dosocilova, J. Polym. Sci., B2, 421 (1964).

55. T. Yoshino, Y. Kikuchi, and J. Komiyama, J. Phys. Chem., 70, 1059 (1966).

56. M. Matsuzaki and T. Sugimoto, J. Polym. Sci., A2, 5, (1320 (1967).

57. a) T. Yoshino, J. Komiyama, and M. Shinomiya, J. Am. Chem. Soc., 86, 4482 (1964); b) T. Yoshino, M. Shinomiya, and J. Kimoyama, J. Am. Chem. Soc., 87, 387 (1965).

58. T. Yoshino and K. Kuno, J. Am. Chem. Soc., 87, 4404 (1965).

59. T. Yoshino and J. Komiyama, J. Am. Chem. Soc., 88, 176 (1966).

60. T. Yoshino and J. Komiyama, J. Polym. Sci., B4, 991 (1966).

61. R.E. Ireland, R.H. Mueller, and A.K. Willard, J. Am. Chem. Soc., 98, 2868 (1976).

62. T.E. Hogen-Esch and J. Smid, J. Am. Chem. Soc., 88, 307, 318 (1966).

63. C.F. Tien and T.E. Hogen-Esch, Macromolecules, 9, 871 (1976).

64. D. Leaver, W.K. Gilson, and J.D.R. Vass, J. Chem. Soc., 1963, 6053.

65. R.E. Dessey, Y. Okuzumi, and A. Chen, J. Am. Chem. Soc., 84, 2899 (1962).

66. C.E. Castro and R.D. Stephens, J. Am. Chem. Soc., 86, 4358 (1964).

67. A.P. Gray, H. Kraus, D.E. Heitmeier, and R.H. Shiley, J. Org. Chem., 33, 3007 (1968).

BIOGRAPHICAL SKETCH

Waylon L. Jenkins was born December 10, 1951 in Atmore, Alabama, and raised in Jay, Florida. After graduation from Jay High School, he attended Pensacola Junior College. He graduated from the University of West Florida in 1973 when he received a Bachelor of Science degree in chemistry, Summa Cum Laude. He won the Monsanto Award from the UWF chemistry faculty.

In September 1973, he entered the Graduate School of the University of Florida.

He is married to the former Carol Jean Campbell.

I certify that I have read this study and that in my opinion it conforms to acceptable standards of scholarly presentation and is fully adequate, in scope and quality, as a dissertation for the degree of Doctor of Philosophy.

T.E. Hogen Esch, Chairman
Associate Professor of Chemistry

I certify that I have read this study and that in my opinion it conforms to acceptable standards of scholarly presentation and is fully adequate, in scope and quality, as a dissertation for the degree of Doctor of Philosophy.

George B. Butler,
Professor of Chemistry

I certify that I have read this study and that in my opinion it conforms to acceptable standards of scholarly presentation and is fully adequate, in scope and quality, as a dissertation for the degree of Doctor of Philosophy.

Wallace S. Brey, Jr.,
Professor of Chemistry

I certify that I have read this study and that in my opinion it conforms to acceptable standards of scholarly presentation and is fully adequate, in scope and quality, as a dissertation for the degree of Doctor of Philosophy.

John A. Zoltewicz,
Professor of Chemistry

I certify that I have read this study and that in my opinion it conforms to acceptable standards of scholarly presentation and is fully adequate, in scope and quality, as a dissertation for the degree of Doctor of Philosophy.

Ronald J. Gordon,
Associate Professor of Chemical Engineering, Medicine, and Surgery

This dissertation was submitted to the Graduate Faculty of the Department of Chemistry in the College of Arts and Sciences and to the Graduate Council, and was accepted as partial fulfillment of the requirements for the degree of Doctor of Philosophy.

June 1978

Dean, Graduate School